LIVER TRANSPLANTATION 14:1718-1724, 2008

ORIGINAL ARTICLE

Liver Regeneration in Donors and Adult Recipients After Living Donor Liver Transplantation

Junko Haga, Motohide Shimazu, Go Wakabayashi, Minoru Tanabe, Shigeyuki Kawachi, Yasushi Fuchimoto, Ken Hoshino, Yasuhide Morikawa, Masaki Kitajima, and Yuko Kitagawa
Department of Surgery, Keio University School of Medicine, Tokyo, Japan

In living donor liver transplantation, the safety of the donor operation is the highest priority. The introduction of the right lobe graft was late because of concerns about donor safety. We investigated donor liver regeneration by the types of resected segments as well as recipients to assess that appropriate regeneration was occurring. Eighty-seven donors were classified into 3 groups: left lateral section donors, left lobe donors, and right lobe donors. Forty-seven adult recipients were classified as either left or right lobe grafted recipients. Volumetry was retrospectively performed at 1 week, 1, 2, 3, and 6 months, and 1 year after the operation. In the right lobe donor group, the remnant liver volume was 45.4%, and it rapidly increased to 68.9% at 1 month and 89.8% at 6 months. At 6 months, the regeneration ratios were almost the same in all donor groups. The recipient liver volume increased rapidly until 2 months, exceeding the standard liver volume, and then gradually decreased to 90% of the standard liver volume. Livers of the right lobe donor group regenerated fastest in the donor groups, and the recipient liver regenerated faster than the donor liver. Analyzing liver regeneration many times with a large number of donors enabled us to understand the normal liver regeneration pattern. Although the donor livers did not reach their initial volume, the donors showed normal liver function at 1 year. The donors have returned to their normal daily activities. Donor hepatectomy, even right hepatectomy, can be safely performed with accurate preoperative volumetry and careful decision-making concerning graft-type selection. *Liver Transpl 14:1718-1724, 2008.* © 2008 AASLD.

Received December 13, 2007; accepted July 19, 2008.

Living donor liver transplantation (LDLT) plays an important role because of cultural attitudes and the scarcity of cadaveric donations in Japan.[1] LDLT involves an ethical problem: because the donor operation is performed on a healthy person, donor safety is the highest priority and requires special attention. LDLT was a treatment first for infants, then for children, and finally for adults. Although a left lobe graft provides enough volume for pediatric recipients, some adult recipients require a right lobe graft. There is little question about donor safety, on the basis of remnant liver volume requirements alone, if only a left lateral section and left lobe graft are procured. It is in the use of a right lobe that issues of donor safety come into play. Several authors have studied donor safety, especially with respect to surgical complications and clinical courses.[2,3] Donor safety from various standpoints should be studied further in order to gain insight into the postoperative recovery pattern of a healthy person and to prevent complications.

Although the human liver can tolerate more than 70% hepatectomy,[4] unfortunately some living donors have died of excessive loss of the liver.[5-7] Precise evaluations of donor liver volume are important in order to prevent unexpected hepatic insufficiency and to evaluate normal liver regeneration, which is still unknown to a great extent. Several authors have studied liver regeneration, mostly in diseased livers.[8,9] Complete and

Abbreviations: CT, computed tomography; GW, graft weight; LD, left lobe donor; LDLT, living donor liver transplantation; LR, left lobe grafted recipient; LSD, left lateral section donor; RD, right lobe donor; RR, right lobe grafted recipient; SLV, standard liver volume.

This research was partially supported by the Ministry of Education, Culture, Sports, Science, and Technology through a Grant-in-Aid for the 21st Century Center of Excellence Program entitled "Establishment of Individualized Cancer Therapy Based on Comprehensive Development of Minimally Invasive and Innovative Therapeutic Methods (Keio University)."

Address reprint requests to Motohide Shimazu, M.D., Ph.D., Hachioji Medical Center Tokyo Medical University, 1163 Tatemachi, Hachioji, Tokyo 1930998, Japan. Telephone: +81-42-665-5611; FAX: +81-42-665-1796; E-mail: shimazu@tokyo-med.ac.jp

DOI 10.1002/lt.21622
Published online in Wiley InterScience (www.interscience.wiley.com).

TABLE 1. Profiles of Donors Who Participated in Postoperative Volumetry

Group	n	Male/Female	Age (Years)*	GW (g)†	Ratio of Volume Scheduled To Be Resected (%)‡
LSD	28	15/13	30.5 ± 4.8	247.1 ± 45.9	20.6 ± 5.0
LD	32	21/11	39.4 ± 13.9	442.5 ± 129.4	34.8 ± 9.6
RD	27	10/17	45.1 ± 11.7	627.7 ± 105.7	54.5 ± 10.2

NOTE: All values are expressed as mean ± standard deviation.
Abbreviations: GW, graft weight; LD, left lobe donor; LSD, left lateral section donor; RD, right lobe donor.
*$P < 0.05$ for LSD versus LD and RD.
†$P < 0.05$ for LSD versus LD and RD and for RD versus LD.
‡RD versus LSD and LD.

TABLE 2. Profiles of Recipients Who Participated in Postoperative Volumetry

Group	n	Male/Female	Age (Years)	Acquired GW (g)*	GW/SLV (%)*
LR	22	9/13	42.6 ± 12.1	470.6 ± 122.4	43.3 ± 10.2
RR	25	19/6	45.0 ± 12.7	639.9 ± 98.7	53.8 ± 9.7

NOTE: All values are expressed as mean ± standard deviation.
Abbreviations: GW, graft weight; LR, left lobe grafted recipient; RR, right lobe grafted recipient; SLV, standard liver volume.
*$P < 0.05$.

prompt liver regeneration occurs in donors and recipients in most circumstances.[10,11] It is clinically important to determine liver regeneration in donors as well as recipients. In the present study, liver regeneration in adult recipients was also evaluated for comparison with normal liver regeneration. Volumetric analysis was performed without consideration of the existence of postoperative complications or the recipient primary disease. Accurate reporting on surgical outcomes and liver regeneration helps to ensure proper informed consent, which is obtained from prospective donors.

Liver regeneration is one of the factors reflecting surgical stress and recovery. If a notable difference in the postoperative clinical course, mainly liver regeneration in this study, is not shown between left lateral section donors (LSDs), left lobe donors (LDs), and right lobe donors (RDs), it would mean that the operation for RDs, as well as that for LSDs and LDs, is safe. The purpose of this study was to evaluate liver regeneration in donor groups with respect to the types of resected segments and in recipients and ensure that appropriate regeneration was occurring in both donors and recipients.

PATIENTS AND METHODS

Patients

Between April 1995 and August 2005, 100 LDLTs were performed at Keio University Hospital. The remnant liver volume in donors and the graft volume in recipients were retrospectively measured by computed tomography (CT) films at 1 week, 1, 2, 3, and 6 months, and 1 year after the operation. Eighty-seven donors and 47 adult recipients were enrolled in this study. Patients without regular CT were excluded from this study. Pediatric recipients were excluded because liver regeneration was compared between donors and recipients who had almost the same body weight. Donors were classified into 3 groups: LSD (n = 28), LD (n = 32), and RD (n = 27). Donors underwent volumetric CT assessment of their livers before LDLT to evaluate the whole liver volume and to determine the graft type. Adult recipients were classified into 2 groups: left lobe grafted recipients (LRs; n = 22) and right lobe grafted recipients (RRs; n = 25). Because the calculation of the degree of liver regeneration was based on the standard liver volume (SLV), recipient SLV was calculated with the following equation: SLV = 706.2 × body surface area + 2.4.[12] The graft type was selected according to criteria described previously.[13] In summary, the graft weight (GW) is to be less than 65% of the donor whole liver volume (ie, the remnant liver volume is to be more than 35% of the donor whole liver volume), and GW is to be more than 35% of recipient SLV, which is enough to maintain sufficient liver function. Donor hepatectomy and recipient transplant procedures were performed as described previously.[14]

Donor and Recipient Profiles

Donor and recipient profiles are summarized in Tables 1 and 2, respectively. Donor and recipient ages ranged from 19 to 65 years and from 19 to 63 years, respectively. The average age in the LSD group was the lowest among the groups, and the individual age in that group ranged from 21 to 38 years. The individual ages in the LD and RD groups ranged from 19 to 65 years and from 21 to 65 years, respectively. No donor received a blood transfusion. The mean length of hospital stay after the

operation was 14.8 ± 7.8, 16.8 ± 8.7, and 15.9 ± 7.8 days in the LSD, LD, and RD groups, respectively. It did not differ significantly between the groups. Although complications prolonged hospital stays, the mortality rate (grade V complications of the Clavien classification)[15] among the donors was zero. The postoperative morbidity rate was 21.8% (n = 19). Major complications were bile leakage, wound infection, and fluid collection. Although 1 donor underwent an operation for wound infection (grade III), all other donors recovered completely with conservative treatment (grade II). All donors are currently alive and have returned to their normal daily activities. Among recipients, no significant age differences were found between the LR and RR groups. Ages ranged from 21 to 59 years and from 19 to 63 years in the LR and RR groups, respectively. The postoperative morbidity rate of recipients was 70.3% (grades II-IV), and the mortality rate (grade V) was 19.2%. Diverse recipient complications affected the length of hospital stay. The mortality and morbidity rates did not differ significantly between the groups.

Volumetric Analysis

The donor whole liver volume, donor remnant liver volume, and recipient grafted liver volume were measured by CT films.[16] In the volumetric study, serial transverse scans were performed from the dome to the most inferior portion of the liver. Each slice of the liver was outlined, and the edge of the region of the liver was traced. The liver images were then uploaded from an image scanner (Seiko Epson, Nagano, Japan) to a computer. The profile of the liver image was traced, and an image processing program [Scion Image (public domain software), Scion Corp., Maryland] calculated the liver area. The liver volume was finally calculated by integration of the images from each liver region. GW was measured immediately after retrieval of the graft. The specific gravity of a normal liver is about 1.0, so the volume is similar to the weight. The donor remnant liver volume (day 0) was calculated as follows: whole liver volume − GW. For all patients, we compared the measured actual liver volume postoperatively with the calculated liver volume to obtain the degree of liver regeneration. This value was expressed as a percentage.

Statistical Analysis

All measured values are expressed as the mean ± standard deviation. Statistical significance ($P < 0.05$) was examined by a paired t test. Statistical analysis was performed with SPSS 14.0 (SPSS, Inc., Chicago, IL).

RESULTS

Remnant Liver Volume and Graft Liver Weight

The actual GW ranged from 166 to 928.7 g. The average percentage of GW/donor whole liver volume was 54.5% even in the RD group. This percentage ranged from 13.7% to 37.4%, from 19.7% to 63.4%, and from 27.0% to 70.5% in the LSD, LD, and RD groups, respectively. Among all groups, GW/donor whole liver volume was more than 65% in only 2 cases, both of which were in the RD group. The percentages of GW/donor whole liver volume in these cases were 66.6% and 70.5%, but those at preoperative volumetry were 63.9% and 64.1%, respectively. The percentages of GW/recipient SLV ranged from 29.7% to 72.4% in the LR group and from 41.3% to 84.4% in the RR group. The GW/recipient SLV ratio was less than 35% in 4 cases, all of which were in the LR group. All 4 of these cases showed more than 35% GW/recipient SLV at preoperative volumetry. When right lobe grafts were transplanted, GW/donor whole liver volume was more than 65%, and in 3 cases, it exceeded 70%. A strong positive correlation ($r = 0.92$) was observed between the estimated graft volume and actual GW (Fig. 1).

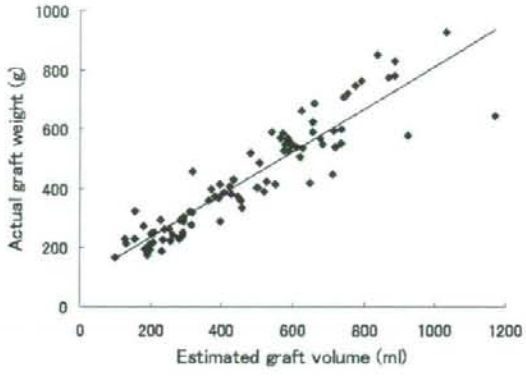

Figure 1. Correlation between the estimated graft volume and actual graft weight. A strong positive correlation was observed between the estimated graft volume and actual graft weight.

Liver Regeneration

Preoperative donor whole liver volume and recipient SLV were regarded as 100% to evaluate the patterns of postoperative liver regeneration, which are shown in Fig. 2. The remnant liver volume of the LSD group was significantly larger than those of the LD and RD groups. The average resected liver volume of the LSD group was about 20% of the whole liver volume. In the RD group, in contrast, the remnant liver volume was 45.4% of the whole liver volume immediately after the operation and then increased rapidly from 68.9% at 1 month to 89.8% at 6 months. At 6 months, the remnant liver volume in the RD group regenerated dramatically, and the regeneration rate was almost the same as those of the LSD and LD groups. In the LSD and LD groups, the liver volume increased gradually until 1 week and then decreased from 1 month to 3 months, reaching around 90% of the preoperative liver volume at 1 year. Among recipients, both the RR and LR groups showed the same regeneration pattern.

Figure 3 shows the patterns of liver regeneration in

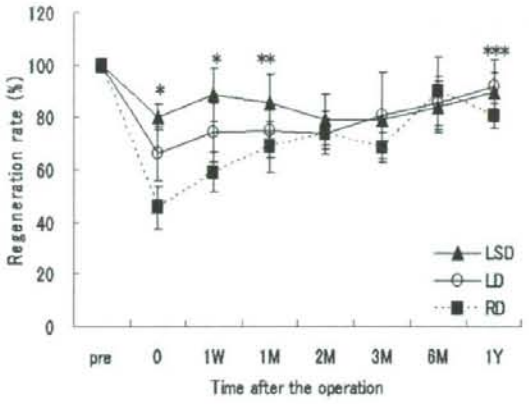

Figure 2. Changes in the remnant liver volume in donors. Rapid liver regeneration was observed in the RD group. A *P* value < 0.05 is shown as follows: *LSD versus LD and RD and LD versus RD, **LSD versus LD and RD, and ***LD versus RD. Abbreviations: LD, left lobe donor; LSD, left lateral section donor; RD, right lobe donor.

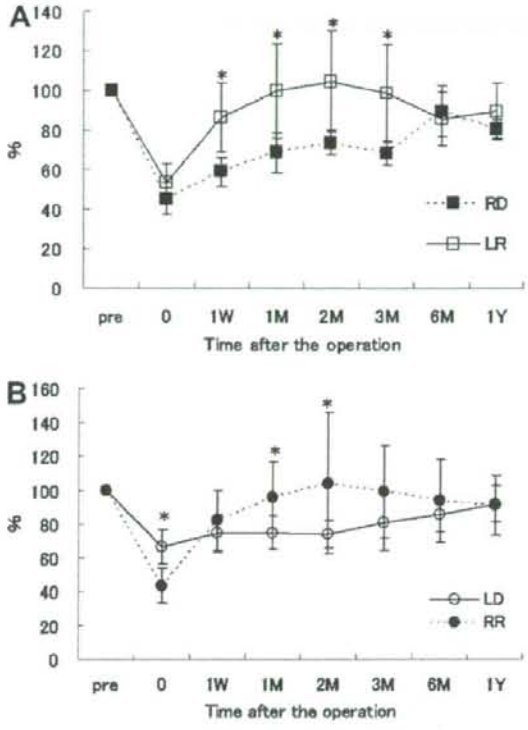

Figure 3. Patterns of liver regeneration in donors and recipients. (A) Donors whose remnant liver is the left lobe (RD) and recipients with a grafted left lobe (LR). (B) Donors whose remnant liver is the right lobe (LD) and recipients with a grafted right lobe (RR). The recipient liver regenerated faster than the donor liver. A *P* value < 0.05 between the donor and recipient is indicated by an asterisk. Abbreviations: LD, left lobe donor; LR, left lobe grafted recipient; RD, right lobe donor; RR, right lobe grafted recipient.

donors and recipients. The same liver segment of each regeneration pattern was evaluated between donors and recipients as follows: (1) the RD group, for which the remnant liver was the left lobe, and the LR group, which received a left lobe graft, and (2) the LD group, for which the remnant liver was the right lobe, and the RR group, which received a right lobe graft. Transplanted grafts regenerated rapidly immediately after LDLT until 2 months, exceeding SLV in both the LR and RR groups. After 2 months, the volume gradually decreased to 90% of SLV. On the other hand, the donor remnant liver volume tended not to reach the preoperative whole liver volume until 1 year. The recipient grafted liver volume increased more rapidly than the donor remnant liver volume, regardless of the type of liver segment.

In Fig. 4, the regeneration rates in donors and recipients who shared the same source of hepatocytes were evaluated as donor-recipient pairs. In this evaluation, the liver volume immediately after the operation, donor remnant liver volume, and recipient grafted liver volume were regarded as 100%. The average regeneration rates in the RD and RR groups were increased from 128.1% ± 20.1% and 165.8% ± 26.0% at 1 week to 159.9% ± 49.6% and 184.7% ± 36.9% at 1 month. The recipient liver regenerated faster than the donor liver. The same result was obtained in the LD and LR groups. The average regeneration rates in the LD and LR groups were increased from 118.0% ± 26.0% and 187.7% ± 32.1% at 1 week to 122.5% ± 24.6% and 200.6% ± 25.2% at 1 month. The less the liver volume was immediately after the operation, the faster the liver regenerated in both the donor and recipient groups.

DISCUSSION

Donor safety is the highest priority because the donor operation is performed on a healthy person in LDLT. Therefore, the preoperative liver volume must be estimated accurately in order to avoid donor death resulting from excessive loss of the liver. LDLT using right lobe grafts was not performed until relatively recently out of concern for donor safety. At Keio University Hospital, adult-to-adult LDLT was started in June 1997, and right lobe graft was first performed in April 1999. A retrospective volumetric study can be performed here because long-term follow-up has been going on for a decade and a large number of LDLTs were performed after the first case of adult-to-adult LDLT.

The LSD group was comparatively young because lateral segment grafts were transplanted to pediatric recipients. These recipients acquired grafts from parents who were younger than the average age of the subjects in this study in most cases. On the other hand, grafts to adult recipients were from their children or elderly parents. This is why the average age of the RD group was high as right lobe grafts were transplanted to adult recipients. The average age differed significantly

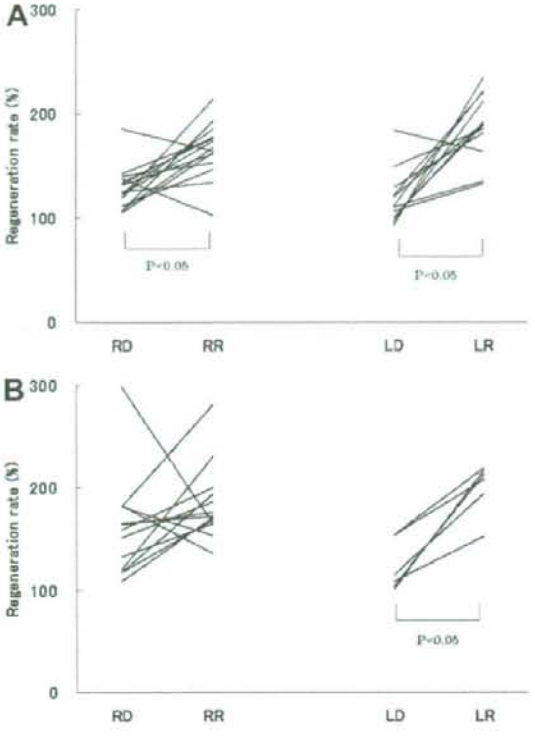

Figure 4. Liver regeneration ratio at (A) 1 week and (B) 1 month after living donor liver transplantation. The lines connect the donor and recipient who share the same source of hepatocytes. Liver volume immediately after the operation was regarded as 100%. In most cases, the regeneration ratio of the recipient liver was higher than that of the donor liver. Abbreviations: LD, left lobe donor; LR, left lobe grafted recipient; RD, right lobe donor; RR, right lobe grafted recipient.

within the donor group but not within the recipient group. Donor age and gender may affect liver regeneration. Some series have reported increased regeneration in younger donors and female donors, possibly secondary to estrogen.[17,18] However, some authors have reported that the liver regeneration rate does not differ by donor age[19] or gender.[20,21] The influences of donor age and gender-related differences on liver regeneration need to be evaluated further.

In this study, liver volume was evaluated by CT. CT is being used as a noninvasive method for evaluating liver vascular anatomy and estimating graft volume. Several types of errors can affect the measurement of liver volume. However, an excellent linear correlation was found between estimated graft volume and actual GW in our study. This means that most of the preoperative graft volume was estimated exactly. With this reliable method, the regeneration of donor remnant livers and that of recipient grafted livers were calculated. CT volumetry revealed that more than 65% of the whole liver volume was resected in 2 donors, and 4 recipients did not gain a graft liver that was more than 35% of their SLV. This implies that these donors and recipients may have insufficient volume to meet their metabolic needs according to our criteria. By preoperative volumetry, these donors and recipients were estimated to have not lost more than 65% of their whole liver volume or to have gained a graft liver less than 35% of their SLV. Thus, if a left lobe graft left the donor with enough liver volume, the recipient did not gain enough liver volume for his or her SLV. In contrast, if a right lobe graft was used to give a recipient sufficient liver volume for his or her SLV, the donor remnant liver volume was too small to meet his or her metabolic demand. For those donors, the liver regenerated sufficiently, and they did not experience liver failure.

The liver regenerates until the liver volume/body weight ratio plateaus. The liver regeneration process has been divided into 3 phases.[22] The early phase is rapid regeneration, which occurs during the first 2 postoperative weeks and is associated with vascular engorgement and tissue edema. The second phase is volume decline, which may be attributable partially to the normalization of developed vascular engorgement or tissue edema at 1 to 2 months after hepatectomy. The third phase is a slow increase in volume, which occurs again until the volume reaches a constant level. In the LSD and LD groups, livers regenerated according to this pattern. In the RD group, the remnant liver continued to regenerate until 2 months without decreasing volume, and volume decline was observed at 3 months. The smaller the remnant liver is, the longer the liver may continue to regenerate up to an extent enough to meet the metabolic needs, regardless of the high regeneration speed. Therefore, the volume decline in the RD group occurred later than those in the LSD and LD groups. Similarly to results published by Nadalin et al.,[23] the RD livers did not return to their full volume but still functioned well without graft failure and with normal liver function at 7 days after the operation. This suggests that livers can function well without returning to the initial volume.

We evaluated adult recipient liver regeneration to reveal how the donor liver regenerates after it was transplanted into recipient, diseased person. The donor and recipient shared the same normal liver parenchyma. Child recipients were excluded because their body size greatly differed from that of the donors. In donor-recipient pairs, the same segment was evaluated, and the source of hepatocytes was the same. The left lobe, which had almost the same liver volume percentage of the whole liver volume immediately after the operation, regenerated faster in recipients than in donors. On the other hand, although the liver volume percentage differed between donors and recipients, the same regeneration pattern observed in the left lobe was observed in the right lobe. The recipient grafted liver regenerated faster than the donor remnant liver regardless of the immediate postoperative volume. Rapid recipient liver regeneration may be related to high liver blood flow after LDLT because of persistence of a hyperdynamic state, immunosuppressant administration, or humoral

factors in the recipient.[10] Cyclosporine[24] and tacrolimus[25] stimulate liver regeneration.

In our previous study, the smaller the liver graft was with respect to the recipient body size and the higher the portal inflow was to it, the more rapidly the liver regenerated after LDLT.[26] Rapid liver regeneration occurred in the small remnant livers and grafts.[27] Several other factors affect liver regeneration, such as the middle hepatic vein,[28] portal venous flow,[26] spleen size,[21] and cytokines.[29,30] The liver regenerates faster with high portal venous flow and preservation of the middle hepatic vein. On the other hand, an enlarged spleen inhibits liver regeneration because an inhibitory protein was released from the spleen cells. Some of the most notable cytokines that induce liver regeneration are hepatocyte growth factor, interleukin-6, and tumor necrosis factor-α. In particular, hepatocyte growth factor plays an important role in liver regeneration. The decline of liver volume induced hepatocyte growth factor production, and liver regeneration was stimulated. Although liver regeneration was evaluated with the exclusion of these factors in the present study, further evaluation considering these factors should reveal in detail the mechanism underlying liver regeneration.

Our retrospective study contributes to our understanding of accurate patterns of normal liver regeneration, which were not evaluated in a previous volumetric study. In this study, liver regeneration was evaluated many times from the preoperative day to 1 year after the operation with a large number of donors. The remnant liver of the RD group, which was smallest, regenerated fastest in the donor group. The donor remnant liver may not regenerate to the full volume that it had before the operation. However, most of the donors achieved normal liver synthetic function within 1 postoperative week and without complications. The difference in liver regeneration between donor and recipient was also comparable. The donor remnant liver seemed to regenerate slowly compared with the recipient grafted liver. An accurate report on liver regeneration as well as liver function helps to ensure proper informed consent. Donor hepatectomy, including right hepatectomy, can be safely performed with accurate preoperative volumetry and careful decision-making concerning graft-type selection because appropriate regeneration occurred and donors showed normal liver function.

REFERENCES

1. Tanaka K, Yamada T. Living donor liver transplantation in Japan and Kyoto University: what can we learn? J Hepatol 2005;42:25-28.
2. Lo CM. Complications and long-term outcome of living liver donors: a survey of 1,508 cases in five Asian centers. Transplantation 2003;75:S12-S15.
3. Fujita S, Kim ID, Uryuhara K, Asonuma K, Egawa H, Kiuchi T, et al. Hepatic grafts from live donors: donor morbidity for 470 cases of live donation. Transpl Int 2000; 13:333-339.
4. Fan ST, Lo CM, Liu CL, Yong BH, Chan JK, Ng IO. Safety of donors in live donor liver transplantation using right lobe grafts. Arch Surg 2000;135:336-340.
5. Akabayashi A, Slingsby BT, Fujita M. The first donor death after living-related liver transplantation in Japan. Transplantation 2004;77:634.
6. Adam R, Lucidi V, Karam V. Liver transplantation in Europe: is there a room for improvement? J Hepatol 2005; 42:33-40.
7. Trotter JF, Wachs M, Everson GT, Kam I. Adult-to-adult transplantation of the right hepatic lobe from a living donor. N Engl J Med 2002;346:1074-1082.
8. Leevy CB. Abnormalities of liver regeneration: a review. Dig Dis 1998;16:88-98.
9. Kitamura T, Watanabe S, Sato N. Liver regeneration, liver cancers and cyclins. J Gastroenterol Hepatol 1998; 13(suppl):S96-S99.
10. Kawasaki S, Makuuchi M, Ishizone S, Matsunami H, Terada M, Kawarazaki H. Liver regeneration in recipients and donors after transplantation. Lancet 1992;339:580-581.
11. Nakagami M, Morimoto T, Itoh K, Arima Y, Yamamoto Y, Ikai I, Yamaoka Y. Patterns of restoration of remnant liver volume after graft harvesting in donors for living related liver transplantation. Transplant Proc 1998;30: 195-199.
12. Urata K, Kawasaki S, Matsunami H, Hashikura Y, Ikegami T, Ishizone S, et al. Calculation of child and adult standard liver volume for liver transplantation. Hepatology 1995;21:1317-1321.
13. Shimazu M, Kitajima M. Living donor liver transplantation with special reference to ABO-incompatible grafts and small-for-size grafts. World J Surg 2004;28:2-7.
14. Kawachi S, Shimazu M, Wakabayashi G, Hoshino K, Tanabe M, Yoshida M, et al. Biliary complications in adult living donor liver transplantation with duct-to-duct hepaticocholedochostomy or Roux-en-Y hepaticojejunostomy biliary reconstruction. Surgery 2002; 132:48-56.
15. Dindo D, Demartines N, Clavien PA. Classification of surgical complications: a new proposal with evaluation in a cohort of 6336 patients and results of a survey. Ann Surg 2004;240:205-213.
16. Yamagishi Y, Saito H, Tada S, Horie Y, Kato S, Ishii H, et al. Value of computed tomography-derived estimated liver volume/standard liver volume ratio for predicting the prognosis of adult fulminant hepatic failure in Japan. J Gastroenterol Hepatol 2005;20:1843-1849.
17. Ikegami T, Nishizaki T, Yanaga K, Shimada M, Kishikawa K, Nomoto K, et al. The impact of donor age on living donor liver transplantation. Transplantation 2000;70:1703-1707.
18. Chiu EJ, Lin HL, Chi CW, Liu TY, Lui WY. Estrogen therapy for hepatectomy patients with poor liver function? Med Hypotheses 2002;58:516-518.
19. Jin MB, Shimamura T, Taniguchi M, Nagasako Y, Suzuki T, Kamiyama T, et al. Liver regeneration in living-donor liver transplantation. Nippon Geka Gakkai Zasshi 2004; 105:674-679.
20. Kwon KH, Kim YW, Kim SI, Kim KS, Lee WJ, Choi JS. Postoperative liver regeneration and complication in live liver donor after partial hepatectomy for living donor liver transplantation. Yonsei Med J 2003;44:1069-1077.
21. Ibrahim S, Chen CL, Wang CC, Wang SH, Lin CC, Liu YW, et al. Liver regeneration and splenic enlargement in donors after living-donor liver transplantation. World J Surg 2005;29:1658-1666.
22. Yamanaka N, Okamoto E, Kawamura E, Kato T, Oriyama T, Fujimoto J, et al. Dynamics of normal and injured human liver regeneration after hepatectomy as assessed on the basis of computed tomography and liver function. Hepatology 1993;18:79-85.
23. Nadalin S, Testa G, Malago M, Beste M, Frilling A,

Schroeder T, et al. Volumetric and functional recovery of the liver after right hepatectomy for living donation. Liver Transpl 2004;10:1024-1029.

24. Mazzaferro V, Porter KA, Scotti-Foglieni CL, Venkataramanan R, Makowka L, Rossaro L, et al. The hepatotropic influence of cyclosporine. Surgery 1990;107:533-539.
25. Starzl TE, Porter KA, Mazzaferro V, Todo S, Fung J, Francavilla A. Hepatotrophic effects of FK506 in dogs. Transplantation 1991;51:67-70.
26. Kato Y, Shimazu M, Wakabayashi G, Tanabe M, Morikawa Y, Hoshino K, et al. Significance of portal venous flow in graft regeneration after living related liver transplantation. Transplant Proc 2001;33:1484-1485.
27. Marcos A, Fisher RA, Ham JM, Shiffman ML, Sanyal AJ, Luketic VA, et al. Liver regeneration and function in donor and recipient after right lobe adult to adult living donor liver transplantation. Transplantation 2000;69:1375-1379.
28. Kido M, Ku Y, Fukumoto T, Tominaga M, Iwasaki T, Ogata S, et al. Significant role of middle hepatic vein in remnant liver regeneration of right-lobe living donors. Transplantation 2003;75:1598-1600.
29. Wakabayashi G, Shimazu M, Ueda M, Tanabe M, Kawachi S, Kitajima M. Liver regeneration after resection: molecular and cellular mechanism. Nippon Geka Gakkai Zasshi 2004;105:650-653.
30. Michalopoulos GK, DeFrances MC. Liver regeneration. Science 1997;276:60-66.

British Journal of Cancer (2008) 99, 1891 – 1899

www.bjcancer.com

Loss of imprinting of *IGF2* correlates with hypermethylation of the *H19* differentially methylated region in hepatoblastoma

S Honda[1,4], Y Arai[2], M Haruta[1], F Sasaki[3], M Ohira[3], H Yamaoka[3], H Horie[3], A Nakagawara[3], E Hiyama[3], S Todo[4] and Y Kaneko[*,1,3]

[1]Department of Cancer Diagnosis, Saitama Cancer Center, Research Institute for Clinical Oncology, 818 Komuro, Ina, Saitama 362-0806, Japan; [2]Cancer Genomics Project, National Cancer Center Research Institute, Chuo-Ku, Tokyo 104-0045, Japan; [3]Japanese Study Group for Pediatric Liver Tumor (JPLT), Hiroshima 734-8551, Japan; [4]Department of General Surgery, Hokkaido University Graduate School of Medicine, Sapporo 060-8638, Japan

IGF2, a maternally imprinted foetal growth factor gene, is implicated in many childhood tumours including hepatoblastoma (HB); however, the genetic and epigenetic alterations have not comprehensively been studied. We analysed the methylation status of the *H19* differentially methylated region (DMR), loss of heterozygosity (LOH) and allelic expression of *IGF2* in 54 *HB* tumours, and found that 12 tumours (22%) with LOH, 9 (17%) with loss of imprinting (LOI) and 33 (61%) with retention of imprinting (ROI). Biallelic and monoallelic *IGF2* expressions correlated with hypermethylation and normal methylation of *H19* DMR, respectively, in two tumours with LOI and seven tumours with ROI. Quantitative RT–PCR analysis showed minimal expression of *H19* mRNA and substantial expression of *IGF2* mRNA in tumours with LOH or LOI, and substantial expression of both *H19* and *IGF2* mRNAs in tumours with ROI. Increased *IGF2* expression with predominant embryonic P3 transcript was found in the majority of HBs with ROI and foetal livers. In contrast to the earlier reports, our findings suggest that the disruption of the enhancer competition model reported in Wilms' tumour may also occur in HB. Both frequencies of LOH and LOI seem to be lower in HB than in Wilms' tumour, reflecting the different tissue origins.

British Journal of Cancer (2008) **99,** 1891 – 1899. doi:10.1038/sj.bjc.6604754 www.bjcancer.com
Published online 28 October 2008

Keywords: hepatoblastoma; *IGF2*; *H19*; loss of heterozygosity; loss of imprinting

Hepatoblastoma (HB) is a rare malignant neoplasm of the liver, with an incidence of 0.5–1.5 per million children (Perilongo and Shafford, 1999). Remarkable progress in clinical outcome has been achieved in the past 20 years because of advances in chemotherapy and surgical procedures; however, the mortality rate remains 20–30% and treatment results in patients in advanced stages who are refractory to standard preoperative chemotherapy regimens are unsatisfactory (Perilongo *et al*, 2000; Fuchs *et al*, 2002). To improve the mortality of these patients, innovative treatment based on a specific molecular target is needed. The molecular mechanism involved in the development and progression of HB includes overexpression of insulin-like growth factor-II (*IGF2*) (Li *et al*, 1998b; Gray *et al*, 2000; Hartmann *et al*, 2000), downregulation of *RASSF1A* by promoter hypermethylation (Sugawara *et al*, 2007; Honda *et al*, 2008) and alterations of genes in the Wnt signalling pathway; most notably, the high incidence of *CTNNB1* (catenin, β1) mutation (Koch *et al*, 1999; Taniguchi *et al*, 2002).

IGF2 is a maternally imprinted gene and encodes a foetal peptide hormone that regulates cellular proliferation and differentiation (Foulstone *et al*, 2005). *IGF2* has four promoter regions and P3 is the most active promoter in the foetal liver, followed by P2 and P4 promoters (Li *et al*, 1998a). *PLAG1* encodes a developmentally regulated transcription factor, which positively regulates *IGF2* through binding the P3 promoter region. Although *IGF2* is downregulated in normal tissues after birth, except for liver tissues, it is overexpressed in a wide variety of childhood and adult cancers and serves as a tumour enhancer through autocrine and paracrine mechanisms (Toretsky and Helman, 1996). *IGF2* has been studied extensively over the past decade as a key molecule involving HB and Wilms' tumour (WT) pathogenesis.

The allelic expression of *IGF2* is regulated by the methylation status of the sixth CTCF (CCCTC-binding factor) site in the *H19* differentially methylated region (DMR) that represents the parental origin of the *IGF2* allele; whereas the paternal CTCF6 allele is methylated, the maternal allele is unmethylated in normal tissues (Bell and Felsenfeld, 2000; Hark *et al*, 2000; Takai *et al*, 2001). Using the enhancer competition model, *IGF2* and *H19* promoters compete on the same chromosome for a shared enhancer, and access of the maternal *IGF2* allele to this enhancer is blocked by *H19* DMR when unmethylated because of the insulator activity of CTCF binding to unmethylated *H19* DMR (Bell and Felsenfeld, 2000; Hark *et al*, 2000). It has been proved in many WTs that aberrant methylation of the maternal CTCF6 prevents the insulator binding and leads to loss of imprinting (LOI), resulting in the overexpression of *IGF2* (Steenman *et al*, 1994; Ravenel *et al*, 2001). Although LOI of *IGF2* was reported in HB, the mechanism of LOI, the concurrent overexpression of *IGF2* mRNA and loss of

*Correspondence: Dr Y Kaneko; E-mail: kaneko@cancer-c.pref.saitama.jp
Received 24 June 2008; revised 30 September 2008; accepted 1 October 2008; published online 28 October 2008

H19 mRNA expression are uncertain because of the limited number of HB tumours examined and the low frequency of the heterozygous *IGF2* polymorphic site in general populations (Davies, 1993; Montagna *et al*, 1994; Rainier *et al*, 1995; Li *et al*, 1995, 1998b; Fukuzawa *et al*, 1999; Gray *et al*, 2000; Hartmann *et al*, 2000; Ross *et al*, 2000; Albrecht *et al*, 2004; Suzuki *et al*, 2008), and some investigators stated earlier that the mechanisms of *IGF2* upregulation by LOI found in WT do not apply to HB (Li *et al*, 1995; Hartmann *et al*, 2000).

Loss of imprinting was reported in 32–38% of WTs (Ravenel *et al*, 2001; Fukuzawa *et al*, 2004; Yuan *et al*, 2005), and loss of heterozygosity (LOH), leading to uniparental disomy (UPD) of the paternal *IGF2*, was reported in 36–50% of WTs (Grundy *et al*, 1996; Fukuzawa *et al*, 2004; Yuan *et al*, 2005). In HB, although LOH of *IGF2* was reported in 20–30%, the incidence of LOI of *IGF2* was uncertain because each series included only a small number of HB tumours. In addition, it is also uncertain whether the same mechanism of LOI is involved in both WT and HB tumorigeneses because the methylation status of *H19* DMR in HB has rarely been examined (Li *et al*, 1995, 1998b; Fukuzawa *et al*, 1999).

To determine whether the alterations of *IGF2* and *H19* loci identified in WT are also found in HB, we examined the LOI and LOH status of *IGF2* using combined bisulphite restriction assay (COBRA) of the CTCF6 region that can determine the methylation status of *H19* DMR more efficiently than the method using methylation-specific restriction enzymes and Southern blot in 54 HB tumours. In addition, we evaluated promoter-specific *IGF2* transcripts, the methylation status of *IGF2* promoters and *PLAG1* mRNA expression. Our results showed that the genetic and epigenetic alterations in the *IGF2-H19* region with elevated expression of *IGF2* mRNA identified in WTs were also found in the great majority of HB tumours, although the incidences of LOH and LOI may be lower in HBs than in WTs.

MATERIALS AND METHODS

Patients and samples

Tumour tissues were obtained from 54 Japanese children with HB, and adjacent normal liver tissues were available from 5 patients. Eighteen tumour and five matched normal liver specimens were supplied by the Tissue Bank of the Japanese Study Group for Pediatric Liver Tumour (JPLT) (Matsunaga *et al*, 2004), and 36 were supplied by institutions affiliated with Saitama Cancer Center. DNA and RNA were extracted from tumour and normal tissue samples that were immediately frozen after the resection or on arrival at the centre. The median age of the 54 patients at diagnosis was 18 months (range, 1–156 months). None of patients had the Beckwith–Wiedemann syndrome or a family history of familial polyposis coli. A total of 14 and 37 tumours were obtained before and after chemotherapy, respectively, and the chemotherapy status was unknown in the other 3 tumours. Pathologists in each institution and/or the JPLT pathology panel made the diagnosis of HB and verified that each sample contained 70% or more tumour cells. Informed consent was obtained from the parents, and the study design was approved by the ethics committee of Saitama Cancer Center.

COBRA of the CTCF6 site at *H19* DMR

We performed COBRA to determine the methylation status of the CTCF6 binding site at *H19* DMR, as described earlier (Watanabe *et al*, 2007). COBRA of CTCF6 showed that the mean methylation percentage ±2 s.d. of five normal livers was 52.8 ± 15.0%, and we defined more than the mean percentage +2 s.d. as the hypermethylated state.

LOH analysis of *IGF2*

High-resolution single nucleotide polymorphism (SNP) array, Affymetrix Mapping 50K-Xba array (Affymetrix, Santa Clara, CA, USA), was used to analyse chromosomal aberrations of 11p15.5 where *IGF2* resides. Genomic DNA in 43 of 54 tumours and 2 cell lines was assayed according to the manufacturer's protocol, and the genomic status of *IGF2* was determined as described earlier (Haruta *et al*, 2008).

Allelic expression analysis of *IGF2* and quantitative real-time reverse transcription-PCR analysis of *IGF2* and *H19* mRNA

The *ApaI*/*AvaII* polymorphic site in exon 9 of *IGF2* was used to evaluate the allelic expression of *IGF2* mRNA in 21 tumours whose RNA was available for this study, as described earlier (Watanabe *et al*, 2006). Quantitative real-time reverse transcription-PCR was performed to evaluate the total *IGF2* and *H19* mRNA levels in 20 tumour tissues, 2 HB cell lines (HuH6 and HepG2), foetal liver total RNA pooled from 34 foetuses (Clontech, Ohtsu, Japan) and 3 normal liver tissues adjacent to HB; the age of the patients was 16, 24 or 26 months. Of the 20 tumours, 3 and 16 were obtained before and after chemotherapy, respectively, and the chemotherapy status was unknown in 1. The primers and TaqMan probes used for *IGF2* and *H19* mRNA were described earlier (Watanabe *et al*, 2007; Haruta *et al*, 2008). The expression of *IGF2* and *H19* mRNAs was normalised with *GAPDH*.

Methylation-specific PCR and bisulphite sequencing analysis of *IGF2* promoter regions

Genomic DNA from tumour and normal liver samples was treated with sodium bisulphite (Herman *et al*, 1996), and the methylation status of the P2–P4 promoter regions of *IGF2* was analysed by methylation-specific PCR (MSP), as described earlier (Beeghly *et al*, 2007). Polymerase chain reaction products were run on 2% agarose gels and visualised after staining with ethidium bromide. We confirmed the results of MSP analysis of P3 promoter by bisulphite sequencing of eight or more subcloned plasmids.

Semiquantitative RT–PCR analysis of promoter-specific transcripts of *IGF2* and *PLAG1*

P1 and P3 promoter specific expressions of *IGF2* mRNA were analysed using the primer sets described elsewhere (Lu *et al*, 2006). The primer sequences for P2-specific transcript were derived from exons 4 and 5: forward, 5′-CCCTCAGGACGTGGACAG-3′; reverse, 5′-GTGCGTTGGACTTGCATAGA-3′; and the primer sequences for P4-specific transcript were derived from exons 7, 8 and 9: forward, 5′-CGAGCCTTCTGCTGAGCTAC-3′; reverse, 5′-CGGAAACAGCA CTCCTCAAC-3′. *PLAG1* mRNA expression was analysed using the following primer sets: forward, 5′-AACGTAAGCGTGGTGAAACC-3′; reverse, 5′-TGCCACATTCTTCGCACTTA-3′ (Zatkova *et al*, 2004). Polymerase chain reaction products were run on polyacrylamide gels and visualised after ethidium bromide staining. The intensity of each band was examined using a fluorescence image analyser, FLA-3000G (Fujifilm, Tokyo, Japan). Dividing the intensity of the target transcript by that of *GAPDH* calculated the level of each transcript.

Mutation analysis of the *CTNNB1* gene

To detect point mutations and deletions of the *CTNNB1* gene, genomic DNA from each tumour sample was amplified using two sets of primers, F1, 5′-TGGCTATCATTCTGCTTTTCTTG-3′ and R1, 5′-CTCTTTTCTTCACCACAACATTTT-3′, and BCAT-3, 5′-AA

AATCCAGCGTGGACAATGG-3′ and BCAT-4, 5′-TGTGGCAAGTT CTGCATCATC-3′, respectively (Koch *et al*, 1999; Satoh *et al*, 2003). The PCR products were either directly sequenced or inserted into a vector (pGEM (R)-T Easy Vector System (Promega, Madison, WI, USA)), and six or more clones were sequenced.

Statistical analysis

Student's *t*-test or Welch's *t*-test compared mRNA levels of *IGF2* and *H19* between tumours with or without *IGF2* alterations or other characteristics and the levels of *IGF2* promoter-specific transcripts between tumours with or without *PLAG1* mRNA expression. We also assessed the association between total *IGF2* mRNA levels and P2-, P3- or P4-specific *IGF2* mRNA levels by determining the Spearman rank correlation coefficient and associated *P*-value. Differences in the incidence of tumours with unmethylated P3 promoter were examined between tumours with hypermethylated *H19* DMR and tumours with normally methylated *H19* DMR by the χ^2 test. Differences in the incidences of tumours with *CTNNB1* mutation were examined between any two of three groups of tumours classified on the basis of the *IGF2* status by the χ^2 test.

RESULTS

Methylation status of the CTCF6 binding site at *H19* DMR, LOH analysis using SNP array and allelic expression analysis of *IGF2*

Combined bisulphite restriction assay showed that 21 and 33 tumours had hypermethylation and normal methylation at CTCF6, indicating LOH or LOI and retention of *IGF2* imprinting (ROI), respectively (Table 1 and Figure 1). Single nucleotide polymorphism array analysis was performed in 43 of 54 tumours; all 21 tumours with hypermethylated CTCF6 and 22 of 33 tumours with normally methylated CTCF6. Combined results of both analyses indicated that 12 tumours had LOH (10 hypermethylated CTCF6 and UPD 2 hypermethylated CTCF6 and hemizygous 11p15 deletion), 9 had LOI (hypermethylated CTCF6 and retention of heterozygosity (ROH)) and 22 had ROI (normally methylated CTCF6 and ROH). Of 21 tumours whose RNA was available, 9 and 12 tumours had heterozygous and homozygous *ApaI*/*AvaII* sites in exon 9 of *IGF2*, respectively. Of the nine heterozygous tumours, seven showed monoallelic expression of *IGF2*, indicating ROI, and two showed biallelic expression of *IGF2*, indicating LOI, and the results were consistent with those examined by COBRA and SNP array analyses (Table 1). From these findings, 11 tumours with normally methylated CTCF6, in which SNP array analysis was not performed, were classified as those with ROI. Thus, combined results of COBRA, SNP array and allelic expression analyses showed 12 tumours with LOH, 9 tumours with LOI and 33 tumours with ROI. In addition, one cell line (HuH6) had LOI, and the other (HepG2) had LOH (UPD) of *IGF2*.

The mean age was compared between any two of three groups of patients (i.e., LOH, LOI or ROI) by Student's *t*-test. There was no difference in the mean age between any two of the three groups of patients.

Correlation between *IGF2* and *H19* mRNA levels and the *IGF2* status (LOH, LOI or ROI)

Quantitative real-time reverse transcription-PCR analysis showed that although 15 of 20 tumours had a higher level of *IGF2* mRNA than normal liver tissues, 15 of 20 tumours had a lower level of *H19* mRNA than normal liver tissues (Table 1 and Figure 2). All 3 tumours with UPD, 1 of 1 with 11p15 loss, 1 of 3 with LOI and 10 of 13 with ROI, expressed higher levels of *IGF2* mRNA than normal liver tissues. There was no significant difference in *IGF2* mRNA levels between 3 tumours with UPD or 7 tumours with *IGF2* alterations; that is UPD, 11p15 loss or LOI, and 13 tumours with ROI. In contrast, 7 tumours with *IGF2* alterations expressed very low levels of *H19* mRNA, whereas 11 of 13 tumours with ROI expressed a substantial amount of *H19* mRNA; 2 tumours (nos. 25 and 27) with ROI expressed very low levels of *H19* mRNA. *H19* mRNA levels were higher in 13 HB tumours with ROI than in 7 HB tumours with *IGF2* alterations ($P<0.01$ by Welch's *t*-test). Although HepG2 with UPD had a higher level of *IGF2* mRNA than normal liver tissues, HuH6 with LOI had a very low level of *IGF2* mRNA. *H19* mRNA levels were very low in both cell lines.

Semiquantitative RT–PCR analysis of promoter-specific *IGF2* transcripts

Because the *IGF2* gene has four kinds of promoters, promoter-specific *IGF2* transcripts were analysed to determine the usage of each promoter. Representative results of the P3 transcript are shown in Figure 3A. All 20 tumours showed undetectable or lower levels of P1 transcripts than 3 normal liver tissues. The levels of P2, P3 and P4 transcripts were higher in 13, 15 and 10 of the 20 tumours, respectively, than those of normal liver tissues. Polymerase chain reaction cycle numbers to obtain visible levels of PCR products were 40 for P2 transcripts, 30 for P3 transcripts and 35 for P4 transcripts, indicating that the amounts of P3 transcripts were high, those of P2 transcripts were low and those of P4 transcripts were intermediate. The Spearman correlation coefficient analysis showed that the expression levels of the P2, P3 and P4 transcripts correlated with the levels of total *IGF2* mRNA (P2, $rS=0.730$; P3, $rS=0.773$ and P4, $rS=0.646$) (Figure 3B and C; data for the P2 and P4 transcripts are not shown).

The methylation status of *IGF2* promoters and its correlation with the levels of promoter-specific transcripts

In the MSP analysis of each promoter, the P2 promoter region was partially methylated in 19 tumours and normal liver tissues and the P4 promoter region was unmethylated in all 20 tumours and normal liver tissues. Therefore, the methylation status of P2 or P4 promoter region was not correlated with the expression level of P2- or P4-specific transcripts. The P3 promoter region was partially methylated in 11 tumours, HuH6 and normal liver tissues and unmethylated in 9 tumours and HepG2 (Table 1, Figure 4A and B). The results of MSP analysis in one tumour (no. 1) and HuH6 were confirmed by bisulphite sequencing (Figure 4C). Nine tumours with the unmethylated P3 promoter had higher levels of P3 transcripts than 11 tumours with the partially methylated P3 promoter ($P=0.005$) (Figure 4D). The P3 promoter was unmethylated in 5 of 7 tumours with *IGF2* alterations; UPD, 11p15 loss or LOI, but in 4 of 13 tumours with ROI. Thus, the incidence of tumours with unmethylated P3 promoter tended to be higher in tumours with hypermethylated *H19* DMR than in tumours with normally methylated *H19* DMR ($P=0.1$).

Semiquantitative RT–PCR analysis of *PLAG1* mRNA

PLAG1 positively regulates *IGF2*, and its expression was detected in 12 tumours, foetal liver RNA and 2 cell lines, but not in 8 tumour and 3 normal liver tissues (Table 1 and Figure 5). The 12 tumours with *PLAG1* mRNA expression showed higher levels of P4-specific *IGF2* transcripts ($P=0.01$) and tended to show higher levels of P3-specific *IGF2* transcripts ($P=0.051$) than the 8 tumours without *PLAG1* expression. There was no significant difference in P2- or P1-specific transcript levels between tumours with and without *PLAG1* mRNA expression.

Table 1 Genetic and epigenetic status of the *IGF2-H19* region in 54 hepatoblastoma tumours

Patients number	Age[a]/sex	Chemo[b]	%methyl CTCF6[c]	11p15 SNP[d]	*ApaI* site[e]	*IGF2* RT-PCR	*IGF2* status[f]	*IGF2* mRNA	P1E[g]	P2M[h]	P2E	P3M	P3E	P4E	*H19* mRNA	*PLAG1* mRNA	*CTNNB1* status[i]
1	48/F	+	82.8	UPD	Homo	ND	UPD	11.3	0.6	MU	17.7	U	7	3.1	0	+	M
2	5/M	−	93.4	UPD	Homo	ND	UPD	3.9	0	MU	0	U	2.1	0.9	0	−	M
3	24/M	+	76.7	UPD	Homo	ND	UPD	3.2	0	MU	2.4	MU	2.3	1.2	0	+	M
4–10	5–96/M6, F1	+6, −1	72–90	UPD	ND	ND	UPD	ND	ND	ND	ND	ND	ND	ND	ND	ND	M4, N3
11	27/M	+	87.8	Loss chr II	Homo	ND	Loss	6.1	0	MU	2.3	U	4.4	1.3	0	+	M
12	24/M	+	81.9	Loss chr II	ND	ND	Loss	ND	ND	ND	ND	ND	ND	ND	ND	ND	M
13	12/F	+	91.4	ROH	Homo	ND	LOI (m)	9.7	0	U	1.1	U	2.3	0.6	0	−	ND
14	16/M	−	86.1	ROH	Homo	ND	LOI (m)	1	0	MU	0.3	U	1.3	0.9	0	−	ND
15	26/F	+	83.1	ROH	Hetero	LOI	LOI (m, p)	0.8	0	MU	0.4	MU	0.6	0.9	0	−	M
16	24/M	+	70.9	ROH	Hetero	LOI	LOI (m, p)	ND	ND	ND	ND	ND	ND	ND	ND	ND	M
17–21	12–84/M4, F1	+1, −3, UK1	71–91	ROH	ND	ND	LOI (m)	ND	ND	ND	ND	ND	ND	ND	ND	ND	M3,N2
22	12/F	+	52.5	ND	Homo	ND	ROI (m)	9.2	0.8	MU	8.4	MU	2.8	2.2	3.5	+	N
23	109/F	+	49.1	ND	Homo	ND	ROI (m)	8.4	0	MU	4.3	U	4.6	2.8	0.5	+	M
24	12/M	−	56.3	ND	Hetero	ROI	ROI (m, p)	7.4	0	MU	13.2	U	4.6	2.4	1.9	+	M
25	15/M	+	55.9	ROH	Hetero	ROI	ROI (m, p)	5.7	0	MU	6.5	MU	5.1	2.2	0	+	ND
26	6/M	UK	51.1	ND	Hetero	ROI	ROI (m, p)	5.6	0.1	MU	4.7	U	1.2	0.5	2.7	+	ND
27	10/M	+	62.1	ROH	Homo	ND	ROI (m)	5	0	MU	0.9	U	5	1.1	0	−	ND
28	29/F	+	61.5	ND	Homo	ND	ROI (m)	3.7	0	MU	1.5	MU	2.5	1.4	2.5	+	M
29	26/M	+	55.4	ND	Homo	ND	ROI (m)	3.1	0.2	MU	9.3	MU	0.4	1.2	0.7	−	M
30	18/M	+	48.7	ND	Hetero	ROI	ROI (m, p)	2.4	0.1	MU	1.2	MU	1.1	1	0.8	−	ND
31	13/M	+	55.3	ND	Hetero	ROI	ROI (m, p)	2.2	0	MU	1.1	MU	1.5	1	0.6	+	N
32	60/F	+	55.7	ND	Hetero	ROI	ROI (m, p)	0.7	0.2	MU	0.2	MU	0.3	0.9	0.4	+	N
33	29/M	+	56.4	ND	Homo	ND	ROI (m)	0.5	1	MU	0.1	MU	0	0.5	1.2	−	M
34	9/M	+	56.7	ND	Hetero	ROI	ROI (m, p)	0.5	0	MU	0	MU	0.1	0.2	0.2	+	M
35–54	4–156/M11, F9	+12, −7, UK1	41–65	ROH	ND	ND	ROI (m)	ND	ND	ND	ND	ND	ND	ND	ND	ND	M11, N9
Normal livers			52.8	ND	ND	ND	ROI (m)	1	1	MU	1	MU	1	1	1	−	
Fetal livers			ND		ND	ND	ND	5.9	0.2	ND	6.4	ND	4.8	1.9	2.4	ND	
HuH6			87.3	ROH	Hetero	LOI	LOI (m, p)	0	0	MU	0	MU	0	0.1	0	+	M
HepG2			89.5	UPD	Homo	ND	UPD (m)	2.4	0	U	1.5	U	5	2.8	0	+	M

F = female; M = male; M = methylated; ROH = retention of heterozygosity; ROI = retention of imprinting; U = unmethylated; ND = not done; UK = unknown. All 20 tumours showed unmethylated promoter 4; UPD, uniparental disomy; loss chr 11, loss of chromosome 11or 11p15; LOI, loss of imprinting. [a]Age in months. [b]Chemo, chemotherapy before surgery; +6, −1 indicates that six and one tumours were treated and untreated, respectively, with chemotherapy before surgery. [c]%methyl CTCF6 indicates % methylated CTCF6 allele. [d]Results of SNP array. [e]Homo, homozygosity at *ApaI/AvaII* site; hetero, heterozygosity. [f]Results of SNP array analysis, methylation analysis of CTCF6 (m) and *ApaI/AvaII* polymorphism site analysis (p). [g]P1E, promoter 1-specific transcript. [h]P2M, the methylation status of promoter 2. [i]*CTNNB1* status: M, mutated; N, normal.

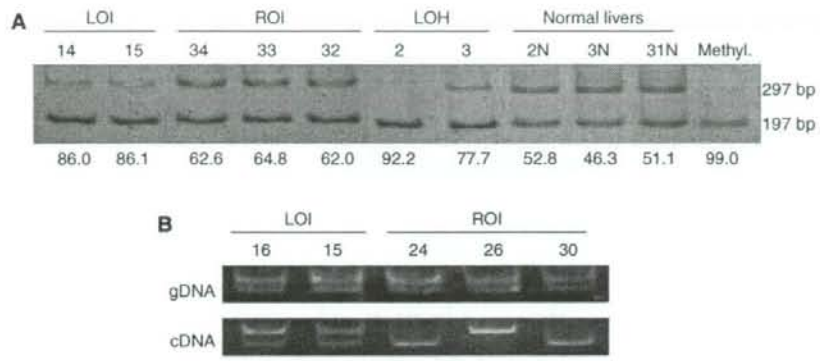

Figure 1 Analysis of *IGF2* alterations. (**A**) Examples of the methylation status of CTCF6 analysed by a combined bisulphite restriction assay (COBRA). Bisulphite-modified PCR products were digested with *MluI*. Upper and lower lanes indicate unmethylated and methylated fragments, respectively. Numbers above lanes indicate the tumour number. Numbers below lanes show the percentage of methylated DNA fragments containing CTCF6. The mean value of the DNA methylation percentages calculated from three COBRA experiments is shown in Table 1. Methyl., control methylated DNA. The *IGF2* status is shown above the tumour numbers. LOI, loss of *IGF2* imprinting; LOH, loss of heterozygosity in the *IGF2* region; ROI, retention of *IGF2* imprinting. (**B**) Electrophoretic pattern of genomic DNA PCR products or RT–PCR products after *AvaII* digestion. Reverse transcriptase–PCR analysis shows LOI in two tumours and ROI in three tumours.

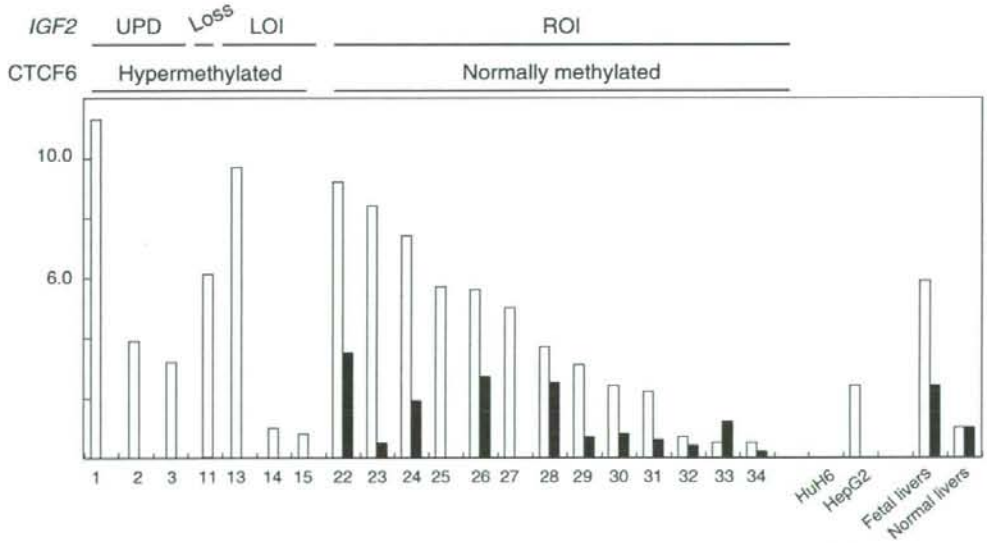

Figure 2 Results of quantitative real-time RT–PCR analysis of *IGF2* and *H19* mRNAs. Relative mRNA (*Y* axis) of total *IGF2* (open rectangles) and *H19* (closed rectangles) is plotted in 3 tumours with UPD, in 1 tumour with 11p15 loss, in 3 tumours with LOI, in 13 tumours with ROI, in 2 cell lines, in foetal liver total RNA and in adjacent normal liver tissues (a mean value of 3 samples). Tumours in each group are arranged in order by the levels of *IGF2* mRNA. Numbers below *X* axis indicate the tumour number shown in Table 1. *IGF2* status (UPD, loss of 11p15, LOI and ROI) and methylation status of CTCF6 at *H19* DMR (hypermethylated or normally methylated) are shown above the graph. Nine tumours (nos. 1–3, 11, 13–15, 25 and 27) and two cell lines expressed a minimal amount of *H19* mRNA, which was shown as zero in the graph. Similarly, HuH6 expressed a minimal amount of *IGF2* mRNA, which was shown as zero in the graph.

Incidences of tumours with *CTNNB1* mutation between any two groups of tumours classified on the basis of the *IGF2* status

DNA was available for *CTNNB1* mutation analysis in 48 of 54 HB tumours. The results are described in Table 1. There were no differences in the incidences of *CTNNB1* mutation between 7 tumours with *IGF2*-LOI and 29 tumours with *IGF2*-ROI or 12 tumours with *IGF2*-LOH, and between 29 tumours with *IGF2*-ROI and 12 tumours with *IGF2*-LOH.

DISCUSSION

In this study, biallelic and monoallelic *IGF2* expressions correlated with hypermethylation and normal methylation of CTCF6,

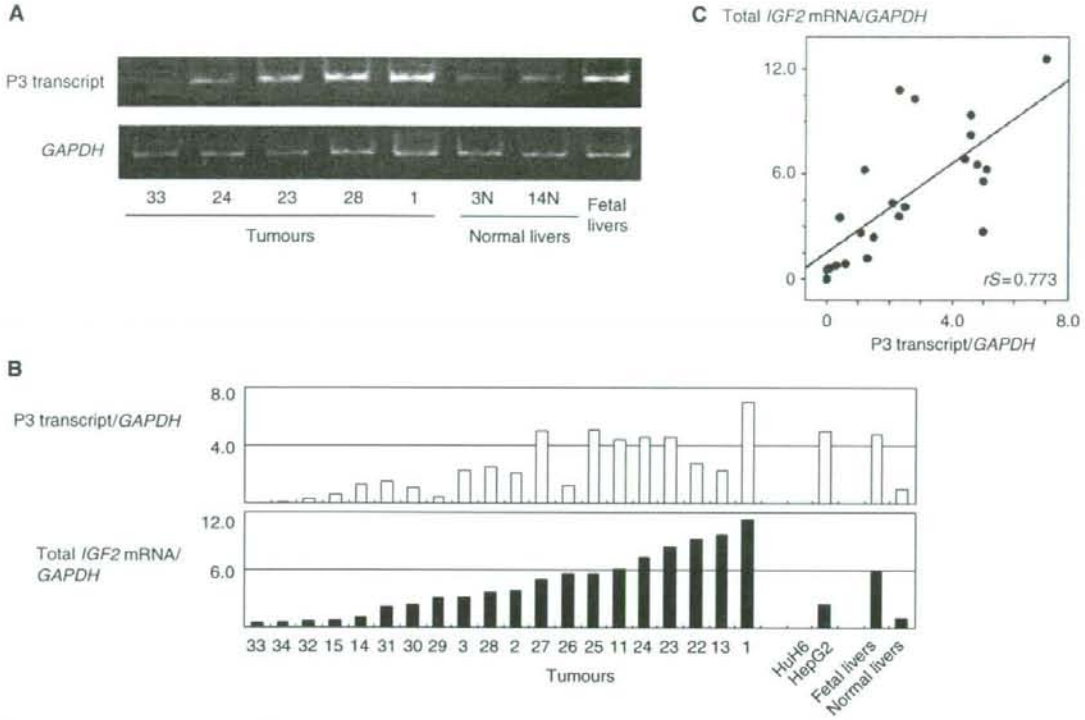

Figure 3 (**A**) Representative data of RT–PCR analysis of P3 transcripts. (**B**) Expression levels of P3 transcripts (upper lane) and total *IGF2* mRNA (lower lane) are plotted in 20 tumours, in 2 cell lines, in foetal liver tissues and normal liver tissues (a mean value of 3 samples). Tumours are arranged in order by total levels of *IGF2* mRNA. Numbers below *X* axis indicate the tumour number. (**C**) Correlation between levels of P3 transcript (*X* axis) and total *IGF2* mRNA (*Y* axis).

respectively, in two tumours with LOI and seven tumours with ROI (Table 1, Figure 1). In addition, the paternal origin of the duplicated *IGF2* loci was confirmed by the hypermethylated CTCF6 in 10 tumours with UPD. Furthermore, very low expression levels of *H19* mRNAs and substantial expression levels of *IGF2* mRNAs in HB tumours with UPD or LOI, and substantial expression levels of both *IGF2* and *H19* mRNA in HB tumours with ROI were found (Table 1 and Figure 2). Two (nos. 14 and 15) of three HB tumours with LOI expressed *IGF2* mRNA levels comparable to but not higher than those of *IGF2* mRNA in normal liver tissues. In addition, one cell line, HuH6, with LOI expressed minimal expression of *IGF2* mRNA, although Hartmann *et al* (2000) found the moderate expression in the same cell line. These findings may be explained by the speculation that such tumours expressed increased levels of *IGF2* mRNA at the critical time of tumorigenesis, but not at the time of surgical resection or after many passages of cell culture. From these findings, the hypothesis established for WT that the hypermethylation of maternal *H19* DMR causes LOI, and that LOI or duplication of paternal *IGF2* (UPD) results in overexpression of *IGF2*, may be also applied to HB.

Although the expression levels of *IGF2* mRNA were reported to be higher in WTs with UPD than in WTs with ROI in two series of WTs (Wang *et al*, 1996; Haruta *et al*, 2008), conflicting results were reported in *IGF2* mRNA levels between WTs with LOI and WTs with ROI (Wang *et al*, 1996; Ravenel *et al*, 2001). The present and earlier studies showed that all HB tumours with UPD and the majority of HB tumours with LOI or ROI expressed the higher levels of *IGF2* mRNA than normal liver tissues (Li *et al*, 1998b; Gray *et al*, 2000; Hartmann *et al*, 2000). This study also showed that P3 transcripts predominated in total *IGF2* mRNAs in HB tumours irrespective of the *IGF2* status (i.e., UPD, 11p15 loss, LOI or ROI); these findings were similar to those reported in foetal liver tissues showing elevated expression of *IGF2* mRNA with predominance of the P3 transcript (Li *et al*, 1998a). Thus, the high *IGF2* mRNA expression of many HB tumours with ROI may mimic the upregulation of *IGF2* expression in embryonic liver tissues, from which HB may arise.

In this study of 54 HB tumours, we found LOH in 12 (22.2%), LOI in 9 (16.7%) and ROI in 33 (61.1%). Hepatoblastoma tumours can be classified into those with LOH and those with ROH, and tumours with ROH can be further classified into those with LOI and those with ROI. For data comparison, the frequencies of LOH and LOI in the earlier and present series of HB tumours are shown in Tables 2 and 3, respectively (Davies, 1993; Montagna *et al*, 1994; Li *et al*, 1995; Rainier *et al*, 1995; Fukuzawa *et al*, 1999; Gray *et al*, 2000; Hartmann *et al*, 2000; Ross *et al*, 2000; Albrecht *et al*, 2004; Suzuki *et al*, 2008). Both frequencies of LOH and LOI were similar between the earlier and present series of HB tumours. When we compared the frequencies of LOH and LOI between HB and WT, the frequencies of LOH and LOI are lower in HB tumours than in WT tumours (Table 4). The present and earlier studies showed that levels of *IGF2* mRNA are higher in normal liver tissues than in normal kidney tissues, and in foetal liver tissues than in foetal kidney tissues, but showed similarly high levels in both WTs and HBs (part of the data not shown) (Hedborg *et al*, 1994; Haruta

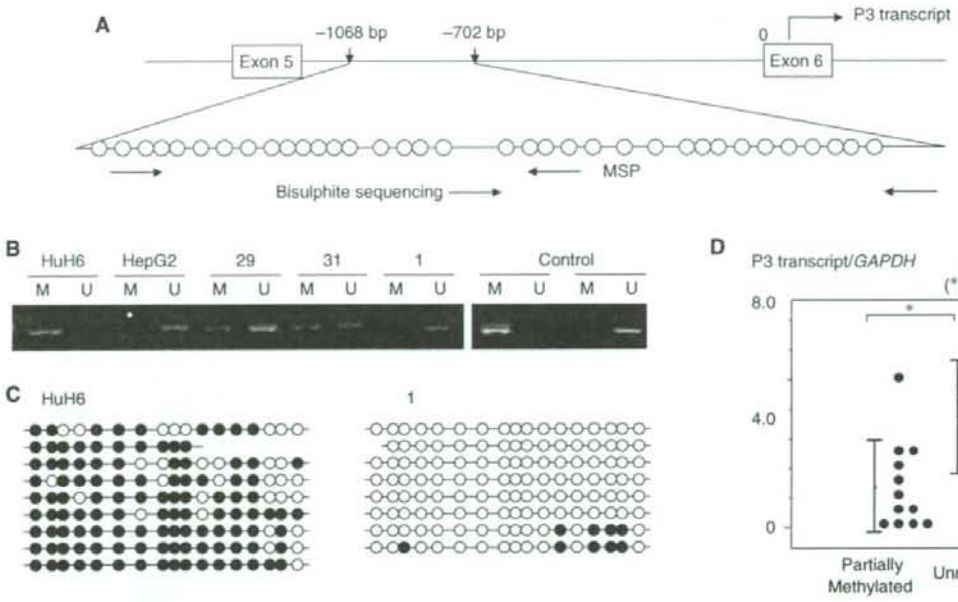

Figure 4 (**A**) Diagram of the *IGF2* P3 promoter region. Individual CpG dinucleotides located upstream of exon 6 (from −1068 to −702 bp) are represented by circles. Horizontal arrows indicate locations of PCR primers used for MSP and bisulphite sequencing. (**B**) Examples of the promoter methylation status using methylation-specific PCR. Polymerase chain reaction products of methylated or unmethylated P3 promoters from HB tumours are shown. Numbers above horizontal bars indicate the tumour number. M, methylated promoter; U, unmethylated promoter. (**C**) Bisulphite sequencing analysis of the methylation status of P3 promoter in HuH6 and one tumour (no. 1), which displayed complete methylation and complete unmethylation, respectively. Open and closed circles indicate unmethylated and methylated CpG dinucleotides, respectively. (**D**) Levels of P3 transcripts in tumours with partially methylated P3 promoter and tumours with unmethylated P3 promoter.

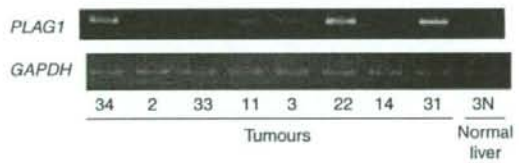

Figure 5 Representative data of RT–PCR analysis of *PLAG1* mRNA. Numbers below lanes indicate the tumour number.

et al, 2008), indicating that embryonal kidney tissues might be more susceptible to IGF2 stimulation than embryonal liver tissues. These findings might be related to higher incidences of UPD or LOI in WT than in HB.

The *IGF2* gene has four promoter regions and each promoter can initiate transcription producing a distinct *IGF2* transcript with different 5′-untranslated regions with a common translated region in the 3′-side (Li *et al*, 1998a). The *IGF2* gene is transcriptionally regulated in a development-dependent and tissue-specific manner. In the foetal liver, promoters P2, P3, and P4 are active and expressed monoallelically; P3 is the most active promoter and P1 is inactive. However, in the adult liver, P1 becomes dominant and is biallelically expressed, and P2, P3 and P4 activities are decreased or lost (Li *et al*, 1998a). In foetal liver tissues, P3 promoter methylation is inversely correlated with the P3 transcript expression. The inverse correlation between P3 promoter methylation and P3 transcript expression was reported earlier in seven HB tumours (Li *et al*, 1998b). This study confirmed the upregulation of P2, P3 and P4 transcripts and downregulation of P1 transcript, and

Table 2 Incidences of LOH of *IGF2* in previous and present series of hepatoblastoma and Wilms' tumours

References	Total number	LOH of *IGF2**	No-LOH of *IGF2*	%
Hepatoblastoma				
Montagna *et al* (1994)	13	3	10	23.1
Fukuzawa *et al* (1999)	7	2	5	28.6
Gray *et al* (2000)	10	2	8	20.0
Hartmann *et al* (2000)	24	6	18	25.0
Albrecht *et al* (2004)	56	13	43	23.2
Suzuki *et al* (2008)	17	4	13	23.5
Total number	127	30	97	23.6
Present study	54	12	42	22.2
Wilms' tumour				
Grundy *et al* (1996)	260	93	167	35.8
Yuan *et al* (2005)	62	26	36	41.9

*Tumours with LOH of 11p15, but no informative *IGF2* locus are included.

the inverse correlation between P3 promoter methylation and P3 transcript expression in the majority of 20 HB tumours. Although P2, P3 and P4 transcripts were all correlated to the total amount of *IGF2* mRNAs, the earlier and present studies showed that the P3 transcript was most abundant and seemed to play a major role in the tumorigenesis of HB (Li *et al*, 1998b). Increased *IGF2* expression with the predominant P3 transcript was reported earlier in WTs with LOI or ROI (Vu and Hoffman, 1999). This study also showed that HB tumours with hypermethylated *H19* DMR tended to have an unmethylated P3 promoter, indicating that

Table 3 Incidences of LOI of *IGF2* in previous and present series of hepatoblastoma and Wilms' tumours

References	Total number[a]	LOI of *IGF2*	ROI of *IGF2*	%
Hepatoblastoma				
Davies (1993)	3	0	3	0
Montagna *et al* (1994)	5	1	4	20.0
Rainier *et al* (1995)	5	1	4	20.0
Li *et al* (1995)	3	1	2	33.3
Fukuzawa *et al* (1999)	4	1	3	25.0
Ross *et al* (2000)	13	3	10	23.1
Hartmann *et al* (2000)	5	3	2	60.0
Total number	38	10	28	26.3
Present study	42	9	33	21.4
Wilms' tumour				
Ravenel *et al* (2001)	36	15	21	41.7
Yuan *et al* (2005)	29	22	7	75.9

[a]Tumours with LOH of *IGF2* were excluded.

Table 4 Incidences of LOH, LOI and ROI of *IGF2* in hepatoblastoma and Wilms' tumours

References	Total number	LOH of *IGF2*	LOI of *IGF2*	ROI of *IGF2*
Hepatoblastoma				
Present study	54	12 (22.2%)	9 (16.7%)	33 (61.1%)
Wilms' tumour				
Fukuzawa *et al* (2004)	41	17 (41.5%)	13 (31.7%)	11 (26.8%)
Yuan *et al* (2005)	58	29 (50.0%)	22 (37.9%)	7 (12.1%)

the paternal P3 promoter or the maternal P3 promoter upstream of the aberrantly methylated *H19* DMR is likely to be unmethylated, probably because of stimulation of the enhancer signal. In contrast, the significance of unmethylation in the P3 promoter found in 4 (nos. 23, 24, 26 and 27) of 13 HB tumours with normally methylated *H19* DMR (ROI) remains unresolved.

PLAG1 located in 8q11 encodes a developmentally regulated transcription factor, and positively regulates *IGF2*. The P3 promoter region of *IGF2* contains *PLAG1* consensus-binding sites, and PLAG1 transactivates the transcription from embryonic *IGF2* promoter P3 in HB cell lines, HuH6 and HepG2 (Zatkova *et al*, 2004). *PLAG1* mRNA was highly expressed in most HB tumours compared with normal liver tissues. In this study, HB tumours with *PLAG1* mRNA expression showed and tended to show higher levels of P4 and P3 transcripts, respectively. Thus, the correlation of *PLAG1* mRNA expression with increased levels of P3 transcripts reported by Zatkova *et al* (2004) may be confirmed; furthermore, the correlation of *PLAG1* mRNA expression with increased levels of P4 transcripts was also suggested.

WTs can be classified at least into two groups; one has intralobar nephrogenic rest that is associated with *WT1* abnormality and the other has perilobar nephrogenic rest associated with *IGF2*-LOI (Ravenel *et al*, 2001). *CTNNB1* mutation is frequently found in WTs with *WT1* abnormality, but rare in WTs without *WT1* abnormality (Maiti *et al*, 2000). These findings suggest that WTs with no *WT1* abnormality may include a substantial number of tumours with *IGF2*-LOI, and that *CTNNB1* mutation and *IGF2*-LOI may be mutually exclusive in WT and also in HB. However, there were no differences in the incidences of *CTNNB1* mutation between HBs with *IGF2*-LOI and those with *IGF2*-ROI, or those with *IGF2*-LOH. We have recently reported a paper describing the occurrence of duplication of paternal *IGF2* or *IGF2*-LOI in half of WTs with *WT1* abnormalities (Haruta *et al*, 2008). Of two WTs with *IGF2*-LOI and *WT1* abnormality reported in that paper, one had *CTNNB1* mutation and the other had not. These findings suggest that *CTNNB1* mutation and *IGF2*-LOI may not be mutually exclusive in either WT or HB.

The IGF signalling pathway is activated in various cancers, and monoclonal antibodies targeting IGF1R have been recently developed; IGF1R is a transmembrane tyrosine kinase receptor, and both IGF1 and IGF2 are ligands for IGF1R (Foulstone *et al*, 2005). Early clinical trials using anti-IGF1R monoclonal antibodies showed promising results in refractory Ewing's sarcomas and rhabdomyosarcomas (Ryan and Goss, 2008). Because 20–30% of HB tumours do not respond to the current chemotherapy consisting of cisplatin and adriamycin (Perilongo *et al*, 2000; Fuchs *et al*, 2002), and the great majority of HB tumours overexpresses *IGF2*, as shown in the present and earlier studies, HB may be the next target tumour for antibody therapy.

ACKNOWLEDGEMENTS

This study was supported by Ministry of Health, Labor and Welfare, Japan for Third-Term Comprehensive Control Research for Cancer (Y Kaneko). We are grateful to Dr K Hiyama, Hiroshima University, a data administrator for JPLT, for data management. We also express our gratitude to the physicians participating in JPLT who supplied samples for this study.

REFERENCES

Albrecht S, Hartmann W, Houshdaran F, Koch A, Gärtner B, Prawitt D, Zabel BU, Russo P, Von Schweinitz D, Pietsch T (2004) Allelic loss but absence of mutations in the polyspecific transporter gene *BWR1A* on 11p15.5 in hepatoblastoma. *Int J Cancer* **111**: 627–632

Beeghly AC, Katsaros D, Wiley AL, Rigault de la Longrais IA, Prescott AT, Chen H, Puopolo M, Rutherford TJ, Yu H (2007) IGF-II promoter methylation and ovarian cancer prognosis. *J Cancer Res Clin Oncol* **133**: 713–723

Bell AC, Felsenfeld G (2000) Methylation of a CTCF-dependent boundary controls imprinted expression of the *Igf2* gene. *Nature* **405**: 482–485

Davies SM (1993) Maintenance of genomic imprinting at the IGF2 locus in hepatoblastoma. *Cancer Res* **53**: 4781–4783

Foulstone E, Prince S, Zaccheo O, Burns JL, Harper J, Jacobs C, Church D, Hassan AB (2005) Insulin-like growth factor ligands, receptors, and binding proteins in cancer. *J Pathol* **205**: 145–153

Fuchs J, Rydzynski J, Von Schweinitz D, Bode U, Hecker H, Weinel P, Bürger D, Harms D, Erttmann R, Oldhafer K, Mildenberger H (2002) Pretreatment prognostic factors and treatment results in children with hepatoblastoma. *Cancer* **95**: 172–182

Fukuzawa R, Breslow NE, Morison IM, Dwyer P, Kusafuka T, Kobayashi Y, Becroft DM, Beckwith JB, Perlman EJ, Reeve AE (2004) Epigenetic differences between Wilms' tumours in white and East-Asian children. *Lancet* **363**: 446–451

Fukuzawa R, Umezawa A, Ochi K, Urano F, Ikeda H, Hata J (1999) High frequency of inactivation of the imprinted *H19* gene in 'sporadic' hepatoblastoma. *Int J Cancer* **82**: 490–497

Gray SG, Eriksson T, Ekström C, Holm S, von Schweinitz D, Kogner P, Sandstedt B, Pietsch T, Ekström TJ (2000) Altered expression of members of the IGF-axis in hepatoblastomas. *Br J Cancer* **82**: 1561–1567

Grundy P, Telzerow P, Moksness J, Breslow NE (1996) Clinicopathologic correlates of loss of heterozygosity in Wilms' tumors: a preliminary analysis. *Med Pediatr Oncol* **27**: 429–433

Hark AT, Schoenherr CJ, Katz DJ, Ingram RS, Levorse JM, Tilghman SM (2000) CTCF mediates methylation-sensitive enhancer-blocking activity at the *H19/Igf2* locus. *Nature* **405:** 486–489

Hartmann W, Waha A, Koch A, Goodyer CG, Albrecht S, von Schweinitz D, Pietsch T (2000) $p57^{KIP2}$ is not mutated in hepatoblastoma but shows increased transcriptional activity in a comparative analysis of the three imprinted genes $p57^{KIP2}$, *IGF2*, and *H19*. *Am J Pathol* **157:** 1393–1403

Haruta M, Arai Y, Sugawara W, Watanabe N, Honda S, Ohshima J, Soejima H, Nakadate H, Okita H, Hata J, Fukuzawa M, Kaneko Y (2008) Duplication of paternal *IGF2* or loss of maternal *IGF2* imprinting occurs in half of Wilms tumors with various structural *WT1* abnormalities. *Genes Chromosomes Cancer* **47:** 712–727

Hedborg F, Holmgren L, Sandstedt B, Ohlsson R (1994) The cell type-specific *IGF2* expression during early human development correlates to the pattern of overgrowth and neoplasia in the Beckwith–Wiedemann syndrome. *Am J Pathol* **145:** 802–817

Herman JG, Graff JR, Myöhänen S, Nelkin BD, Baylin SB (1996) Methylation-specific PCR: a novel PCR assay for methylation status of CpG islands. *Proc Natl Acad Sci USA* **93:** 9821–9826

Honda S, Haruta M, Sugawara W, Sasaki F, Ohira M, Matsunaga T, Yamaoka H, Horie H, Ohnuma N, Nakagawara A, Hiyama E, Todo S, Kaneko Y (2008) The methylation status of *RASSF1A* promoter predicts responsiveness to chemotherapy and eventual cure in hepatoblastoma patients. *Int J Cancer* **123:** 1117–1125

Koch A, Denkhaus D, Albrecht S, Leuschner I, Von Schweinitz D, Pietsch T (1999) Childhood hepatoblastomas frequently carry a mutated degradation targeting box of the β-catenin gene. *Cancer Res* **59:** 269–273

Li X, Adam G, Cui H, Sandstedt B, Ohlsson R, Ekström TJ (1995) Expression, promoter usage and parental imprinting status of insulin-like growth factor II (*IGF2*) in human hepatoblastoma: uncoupling of *IGF2* and *H19* imprinting. *Oncogene* **11:** 221–229

Li X, Gray SG, Flam F, Pietsch T, Ekström TJ (1998a) Developmental-dependent DNA methylation of the *IGF2* and *H19* promoters is correlated to the promoter activities in human liver development. *Int J Dev Biol* **42:** 687–693

Li X, Kogner P, Sandstedt B, Haas OA, Ekström TJ (1998b) Promoter-specific methylation and expression alterations of *igf2* and *h19* are involved in human hepatoblastoma. *Int J Cancer* **75:** 176–180

Lu L, Katsaros D, Wiley A, Rigault de la Longrais IA, Puopolo M, Schwartz P, Yu H (2006) Promoter-specific transcription of insulin-like growth factor II in epithelial ovarian cancer. *Gynecol Oncol* **103:** 990–995

Maiti S, Alam R, Amos CI, Huff V (2000) Frequent association of *β-catenin* and *WT1* mutations in Wilms tumors. *Cancer Res* **60:** 6288–6292

Matsunaga T, Sasaki F, Ohira M, Hashizume K, Hayashi A, Hayashi Y, Matsuyama K, Mugishima H, Ohnuma N (2004) The role of surgery in the multimodal treatment for hepatoblastomas. *Shounigan* **41:** 205–210 (in Japanese)

Montagna M, Menin C, Chieco-Bianchi L, D'Andrea E (1994) Occasional loss of constitutive heterozygosity at 11p15.5 and imprinting relaxation of the *IGFII* maternal allele in hepatoblastoma. *J Cancer Res Clin Oncol* **120:** 732–736

Perilongo G, Shafford EA (1999) Liver tumours. *Eur J Cancer* **35:** 953–958

Perilongo G, Shafford S, Plaschkes J (2000) SIOPEL trials using preoperative chemotherapy in hepatoblastoma. *Lancet Oncol* **1:** 94–100

Rainier S, Dobry CJ, Feinberg AP (1995) Loss of imprinting in hepatoblastoma. *Cancer Res* **55:** 1836–1838

Ravenel JD, Broman KW, Perlman EJ, Niemitz EL, Jayawardena TM, Bell DW, Haber DA, Uejima H, Feinberg AP (2001) Loss of imprinting of insulin-like growth factor-II (IGF2) gene in distinguishing specific biologic subtypes of Wilms tumor. *J Natl Cancer Inst* **93:** 1698–1703

Ross JA, Radloff GA, Davies SM (2000) *H19* and *IGF-2* allele-specific expression in hepatoblastoma. *Br J Cancer* **82:** 753–756

Ryan PD, Goss PE (2008) The emerging role of the insulin-like growth factor pathway as a therapeutic target in cancer. *Oncologist* **13:** 16–24

Satoh Y, Nakagawachi T, Nakadate H, Kaneko Y, Masaki Z, Mukai T, Soejima H (2003) Significant reduction of *WT1* gene expression, possibly due to epigenetic alteration in Wilms' tumor. *J Biochem* **133:** 303–308

Steenman MJ, Rainier S, Dobry CJ, Grundy P, Horon IL, Feinberg AP (1994) Loss of imprinting of *IGF2* is linked to reduced expression and abnormal methylation of *H19* in Wilms tumor. *Nat Genet* **7:** 433–439

Sugawara W, Haruta M, Sasaki F, Watanabe N, Tsunematsu Y, Kikuta A, Kaneko Y (2007) Promoter hypermethylation of the *RASSF1A* gene predicts the poor outcome of patients with hepatoblastoma. *Pediatr Blood Cancer* **49:** 240–249

Suzuki M, Kato M, Yuyan C, Takita J, Sanada M, Nannya Y, Yamamoto G, Takahashi A, Ikeda H, Kuwano H, Ogawa S, Hayashi Y (2008) Whole-genome profiling of chromosomal aberrations in hepatoblastoma using high-density single-nucleotide polymorphism genotyping microarrays. *Cancer Sci* **99:** 564–570

Takai D, Gonzales FA, Tsai YC, Thayer MJ, Jones PA (2001) Large scale mapping of methylcytosines in CTCF-binding sites in the human *H19* promoter and aberrant hypomethylation in human bladder cancer. *Hum Mol Genet* **10:** 2619–2626

Taniguchi K, Roberts LR, Aderca IN, Dong X, Qian C, Murphy LM, Nagorney DM, Burgart LJ, Roche PC, Smith DI, Ross JA, Liu W (2002) Mutational spectrum of beta-catenin, *AXIN1*, and *AXIN2* in hepatocellular carcinomas and hepatoblastomas. *Oncogene* **21:** 4863–4871

Toretsky JA, Helman LJ (1996) Involvement of IGF-II in human cancer. *J Endocrinol* **149:** 367–372

Vu TH, Hoffman AR (1999) Alterations in the promoter-specific imprinting of insulin-like growth factor-II gene in Wilms tumor. *J Biol Chem* **271:** 9014–9023

Wang WH, Duan JX, Vu TH, Hoffman AR (1996) Increased expression of the insulin-like growth factor-II gene in Wilms' tumor is not dependent on loss of genomic imprinting or loss of heterozygosity. *J Biol Chem* **271:** 27863–27870

Watanabe N, Haruta M, Soejima H, Fukushi D, Yokomori K, Nakadate H, Okita H, Hata J, Fukuzawa M, Kaneko Y (2007) Duplication of the paternal *IGF2* allele in trisomy 11 and elevated expression levels of *IGF2* mRNA in congenital mesoblastic nephroma of the cellular or mixed type. *Genes Chromosomes Cancer* **46:** 929–935

Watanabe N, Nakadate H, Haruta M, Sugawara W, Sasaki F, Tsunematsu Y, Kikuta A, Fukuzawa M, Okita H, Hata J, Soejima H, Kaneko Y (2006) Association of 11q loss, trisomy 12, and possible 16q loss with loss of imprinting of insulin-like growth factor-II in Wilms tumor. *Genes Chromosomes Cancer* **45:** 592–601

Yuan E, Li CM, Yamashiro DJ, Kandel J, Thaker H, Murty VV, Tycko B (2005) Genomic profiling maps loss of heterozygosity and defines the timing and stage dependence of epigenetic and genetic events in Wilms' tumors. *Mol Cancer Res* **3:** 493–502

Zatkova A, Rouillard JM, Hartmann W, Lamb BJ, Kuick R, Eckart M, von Schweinitz D, Koch A, Fonatsch C, Pietsch T, Hanash SM, Wimmer K (2004) Amplification and overexpression of the *IGF2* regulator *PLAG1* in hepatoblastoma. *Genes Chromosomes Cancer* **39:** 126–137

MOLECULAR CARCINOGENESIS 47:660–666 (2008)

BRIEF COMMUNICATION

Combined BubR1 Protein Down-Regulation and *RASSF1A* Hypermethylation in Wilms Tumors With Diverse Cytogenetic Changes

Masayuki Haruta,[1]* Yoshiyuki Matsumoto,[2] Hideki Izumi,[2] Naoki Watanabe,[1] Masahiro Fukuzawa,[3] Shinya Matsuura,[2] and Yasuhiko Kaneko[1,3]

[1]*Research Institute for Clinical Oncology, Saitama Cancer Center, Ina, Saitama, Japan*
[2]*Research Institute for Radiation Biology and Medicine, Hiroshima University, Hiroshima, Hiroshima, Japan*
[3]*Japan Wilms Tumor Study Group, Itabashi-Ku, Tokyo, Japan*

BUB1B and *RASSF1A* genes play specific roles in the mitotic checkpoint, and their defects may cause chromosome instability or aneuploidy in mouse fibroblasts and human cancer cell lines; however, few studies have reported a correlation between defects in these genes and chromosome changes in human tumor samples. We examined chromosome abnormalities in 25 Wilms tumors by metaphase comparative genomic hybridization, and classified them into 14 hyperdiploid (50 ≥ chromosomes), 2 near-or-pseudodiploid, and 9 diploid tumors. We also examined various molecular aspects of *BUB1B* and *RASSF1A*, and evaluated the relationship between chromosome changes and the status of both genes. No tumors showed *BUB1B* mutation. BubR1 protein (*BUB1B* gene product) expression was undetectable or decreased in five of six hyperdiploid or near-or-pseudodiploid tumors and increased in four of five diploid tumors, whereas all seven tumors examined showed *BUB1B* mRNA expression irrespective of their chromosome pattern. Furthermore, while complete promoter methylation of *RASSF1A* was found in 13 of 16 hyperdiploid or near-or-pseudodiploid tumors, unmethylated *RASSF1A* was found in 5 of 9 diploid tumors. Partial *RASSF1A* methylation was found in three hyperdiploid or near-or-pseudodiploid tumors and in four diploid tumors. Thus, BubR1 protein expression decreased, and the promoter region of *RASSF1A* was completely methylated in the great majority of hyperdiploid or near-or-pseudodiploid tumors, BubR1 protein expression increased and *RASSF1A* was unmethylated in the majority of diploid tumors. These findings suggest that the combined BubR1 protein down-regulation and *RASSF1A* hypermethylation might be implicated in the formation of chromosomal changes found in Wilms tumors.

Key words: Wilms tumor; *BUB1B*; BubR1 protein expression; *RASSF1A* hypermethylation; chromosome changes

INTRODUCTION

Aneuploidy is a hallmark of cancer, and defects in mitotic checkpoint genes may cause aneuploidy and might promote tumorigenesis [1]. Mouse fibroblasts with reduced levels of Mad1, Mad2, Bub1b, or Bub3 have shown chromosomal instability, and significant increases in the number of aneuploid cells [2–5]. *RASSF1A*, whose promoter methylation is frequently found in various cancers, including Wilms tumor, regulates the stability of mitotic cyclins and the timing of mitotic progression, and its defect caused centrosome abnormalities and multipolar spindles in human cancer cell lines [6–9].

Recently, homozygous and heterozygous mutations of *BUB1B* were found in mosaic variegated aneuploidy (MVA) and premature chromatid separation (PCS) syndromes, respectively, which were clinically characterized by severe intrauterine growth retardation, microcephaly, and eye anomalies [10–12]. Patients with each syndrome are prone to develop Wilms tumor and rhabdomyosarcoma. Karyotypes of two Wilms tumors occurring in patients with PCS syndrome were reported, and showed hyperdiploidy with nonrandom extra chromosomes [13]. We have previously proposed that hyperdiploid Wilms tumors with 50 or more chromosomes may be a genetic subgroup of Wilms tumor characterized by

Abbreviations: PCS, premature chromatid separation; mCGH, metaphase comparative genomic hybridization; RT, reverse-transcription; MSP, methylation-specific PCR; SNP, single-nucleotide polymorphism.

*Correspondence to: Research Institute for Clinical Oncology, Saitama Cancer Center, Komuro 818, Ina, Kitaadachi-gun, Saitama 362-0806, Japan.

Received 11 March 2007; Revised 16 November 2007; Accepted 20 November 2007

DOI 10.1002/mc.20412

Published online 19 February 2008 in Wiley InterScience (www.interscience.wiley.com)

nonrandom extra chromosomes and the absence of *WT1* deletions/mutations [14].

As hyperdiploid Wilms tumor developed in patients with PCS syndrome, we speculated that *BUB1B* mutation might be involved in the neoplastic process of sporadic hyperdiploid Wilms tumor. In addition, although the reduced expression of mitotic checkpoint genes caused chromosomal aneuploidy in mice [2–5], few studies have reported the relationship between chromosomal changes and genetic and epigenetic alterations of the mitotic checkpoint genes in human cancer samples. Thus, we examined mutations and protein expression levels of the *BUB1B* gene and the methylation status of the promoter region of *RASSF1A* in diploid, near-or-pseudodiploid and hyperdiploid Wilms tumors. While undetectable or decreased protein expression levels of BubR1 and complete promoter methylation of *RASSF1A* were found in the great majority of hyperdiploid or near-or-pseudodiploid tumors, increased protein expression levels of BubR1 and unmethylation of *RASSF1A* were found in the majority of diploid tumors. These findings suggest that down-regulation of the BubR1 protein expression and promoter hypermethylation of *RASSF1A* might be related to the chromosome changes found in the majority of Wilms tumors.

MATERIALS AND METHODS

Patient Samples

Tumor samples were obtained from 25 Japanese infants or children ranging in age from 2 months to 15 yr who underwent surgery or biopsy between August 1984 and February 2003. Patients were selected based on the availability of tumor DNA, RNA, and protein. All 25 tumors were diagnosed as Wilms tumor of favorable histology [15]. One patient (No. 17) had Wilms tumor associated with aniridia, and/or genitourinary malformation (WAGR syndrome), and the remaining 24 patients had a sporadic unilateral tumor. Two normal kidney tissue samples adjacent to a Wilms tumor were obtained from 2 patients whose tumor samples were not included in the 25 tumors described above.

Metaphase Comparative Genomic Hybridization (mCGH) Studies

mCGH analysis was performed also as described previously [16]. A chromosomal region was considered to be overrepresented or underrepresented if the average ratio profile was above 1.25 or below 0.75, respectively.

Mutation Analyses of *WT1* and *BUB1B*

Mutational analysis of *WT1* was performed as described previously [14]. PCR primers used for *BUB1B* mutational analysis were designed to amplify all coding exons of *BUB1B* and at least 50 bp of the intronic sequences that contained 5′ and 3′ splice junctions [12]. PCR products were directly sequenced on a sequencer (Applied Biosystems, Foster City, CA).

Western Blot Analysis of BubR1

Western blot analysis using rabbit anti-BubR1 polyclonal antibody raised against human BubR1 (amino acids 1–478) was performed as described previously [12]. α-tubulin detected by mouse anti α-tubulin monoclonal antibody (Sigma–Aldrich, St. Louis, MO) was used as a control for protein loading. Protein extracted from human immortalized skin fibroblast cells was used as a positive control of BubR1. The experiment was performed at least twice, and the results are summarized in Table 1 and Figure 1.

Reverse-Transcription (RT)-PCR Analysis of *BUB1B*

First strand cDNA synthesis was carried out with PrimeScript™ 1st strand cDNA synthesis kit (TAKARA, Ohtsu, Japan) according to the manufacturer's protocol. The PCR was performed with AmpliTaq Gold (Applied Biosystems). PCR primers used were reported previously [17]. PCR products were analyzed by electrophoresis in a 2.0% agarose gel and stained with ethidium bromide (Sigma–Aldrich).

Methylation-Specific PCR (MSP), Bisulfite DNA Sequencing and Quantitative Methylation Analysis of the *RASSF1A* Promoter Region

Genomic DNA from tumor and normal kidney samples was treated with sodium bisulfite as previously described [18]. Bisulfite-modified DNA was amplified as previously described with primers specific for methylated and unmethylated sequences of *RASSF1A* gene promoter regions [18]. Normal lymphocyte DNA treated or untreated with *Sss*I methyltransferase (New England Biolabs, Ipswich, MA) was used as a control for methylated or unmethylated templates, respectively. The amplification primers used for bisulfite DNA sequencing were previously reported. PCR products were inserted into the vectors, and 10 clones from each tumor DNA were sequenced.

Quantitative methylation analysis was performed using LightCycler TaqMan Master on the LightCycler Carousel-Based System (Roche Diagnostics, Alameda, CA) according to the manufacturer's protocol. The actin beta gene (*ACTB*) was used as an internal reference to control for input DNA. The primers and probes used for *RASSF1A* and *ACTB* quantification, and PCR conditions were previously reported [19,20]. Differences in the average quantity of methylated templates between tumors with complete *RASSF1A* methylation and those with partial *RASSF1A* methylation were examined by Student's *t*-test and Welch's *t*-test.

Table 1. BubR1 Protein and *BUB1B* mRNA Expression and Methylation and mRNA Expression Status of *RASS1A* in Wilms Tumors Classified by Metaphase CGH Pattern

				RASSF1A		
Tumor number	Metaphase CGH pattern	BubR1 protein expression	*BUB1B* mRNA	MSP	Quantification	mRNA
Hyperdiploid tumors (≥50 chromosomes) ($n = 14$)						
1	enh(1q, 2, 4, 6, 12), dim(1p13-1pter, 3p, 11, 13q14-qter)	+	ND	M	0.34	ND
2	enh(1q, 2, 6, 7q21-qter, 8, 10, 12pter-q23, 13, 15), dim(1p, 18p)	±	ND	M	0.42	ND
3	enh(1q, 7, 10, 12, 13), dim(11q22-qter)	−	+	M	0.32	−
4	enh(1q, 2, 7, 12, 20)	−	+	M	0.36	−
5	enh(1q, 6, 8, 9, 10, 12, 17, 18)	±	ND	M	0.72	ND
6–11	Various changes	ND	ND	M	0.62, 0.65, 0.66, 0.37, 0.65, 0.85	ND
12–14	Various changes	ND	ND	M + U	0.22, 0.40, 0.30	ND
Near-or-pseudodiploid tumors ($n = 2$)						
15	enh(7q),dim(7p)	−	+	M	0.60	±
16	enh(12),dim(9, 10p, 11q, 16q, 18p)	ND	ND	M	0.64	ND
Diploid tumors ($n = 9$)						
17[a]	Normal	++	ND	M + U	0.34	ND
18	Normal	++	ND	U	0	ND
19	Normal	++	ND	M + U	0.23	ND
20[b]	Normal	++	+	M + U	0.29	−
21	Normal	+	+	M + U	0.39	−
22, 22	Normal	ND	ND	U	0, 0	ND
24, 25	Normal	ND	+	U	0, 0	+
Two normal kidney tissues		−	−	U	0, 0	+
Fetal kidney tissues		ND	−	ND	ND	ND
Human immortalized skin fibroblast cells		++	+	ND	ND	ND

ND, not done; M, methylated band only; M + U, methylated and unmethylated bands; U, unmethylated band only.
[a]The tumor that occurred in a WAGR patient had a hemizygous deletion and a point mutation in exon 8 of *WT1*.
[b]The tumor that occurred in a sporadic patient had a hemizygous deletion and a point mutation in exon 10 of *WT1*.

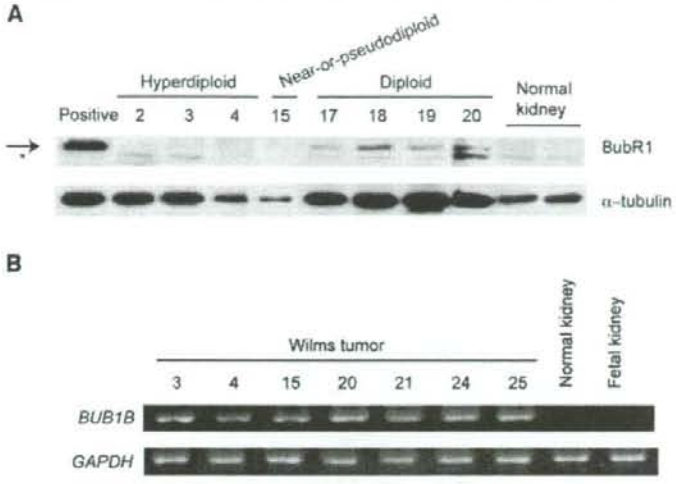

Figure 1. Examples of BubR1 protein and *BUB1B* mRNA expression in Wilms tumors. (A) Western blot showed BubR1 protein and non-specific staining, indicated by an arrow and asterisk, respectively. (B) RT-PCR showed *BUB1B* mRNA expression in all Wilms tumor tissues with various karyotypes, but not in a normal kidney tissue and fetal kidney RNA.

RT-PCR Analysis of *RASSF1A*

RT-PCR analysis of *RASSF1A* was performed as previously described [18].

RESULTS AND DISCUSSION

In mCGH analysis of 25 Wilms tumors, 14 had hyperdiploidy (≥50 chromosomes), 2 had near-or-pseudodiploidy, and 9 had normal diploidy (Table 1). In subsequent sequence analysis of whole exons of the *BUB1B* gene, no mutation was found in all 25 tumors. We found a single-nucleotide polymorphism (SNP), 1064G/A or G > A (rs1601375) at exon 8 of *BUB1B* in 15, and another SNP, 1164G/A or G > A at exon 9 in 4 of the 25 tumors. Four tumors showed heterozygosity only at the SNP site in exon 8, 2 tumors only at the SNP site in exon 9, and one tumor at both sites. Thus, seven tumors retained heterozygosity at the *BUB1B* locus. mCGH analysis showed that the remaining 16 tumors with homozygosity at the locus showed no loss of chromosome 15, supporting that no hemizygous deletion occurred at the locus. Karyotypes of 2 Wilms tumors in patients with PCS syndrome were reported, and showed hyperdiploidy with 48–55 chromosomes, including extra chromosomes 6, 8, 12, 13, 15, 17, and 18 [13]. These karyotypes were similar to those found in hyperdiploid Wilms tumors developed in sporadic patients [14]. Therefore, we speculated that hyperdiploid Wilms tumors of sporadic origin might have *BUB1B* mutations; however, no mutation of the gene was found in either hyperdiploid or non-hyperdiploid tumors. Hanks et al. [21] recently reported no mutation of *BUB1B* in 30 sporadic Wilms tumors although they did not show cytogenetic data, and the present findings were consistent with theirs.

Epigenetic silencing of cancer-related genes is an important mechanism for the development and progression of cancer [22], and one study reported epigenetic down-regulation of *BUB1B* mRNA in some colorectal cancers [23]. In the present study, we examined protein expression levels of BubR1 in 11 Wilms tumors with Western blotting, and showed undetectable or decreased protein expression levels of BubR1 in 5 of 6 hyperdiploid or near-or-pseudodiploid tumors, increased expression levels in 4 of 5 diploid tumors and human immortalized skin fibroblast cells, and undetectable expression levels in two control normal kidney tissues (Table 1 and Figure 1A). Contrary to these findings, *BUB1B* mRNA, which was undetectable in normal and fetal kidney (Clontech, Ohtsu, Japan) tissues, was expressed in all Wilms tumors irrespective of their chromosome pattern (Table 1 and Figure 1B). These findings indicate that BubR1 and *BUB1B* mRNA may be expressed in diploid Wilms tumors, as previously reported in most breast cancer tissues, probably because of the predominance of proliferating cells [17,24]. In contrast, *BUB1B* mRNA may be expressed, but BubR1 may be down-regulated subsequent to the neoplastic transformation of hyperdiploid or near-or-pseudodiploid